Chapter 11
Frequency Planning Techniques

This chapter considers cellular frequency planning techniques for TDMA and OFDMA based cellular systems. System concepts for CDMA cellular systems will be covered in Chap. 12. However, some schemes for high capacity, such as cell sectoring, are flexible enough to be applied to any standard. Regardless of the chosen access method, the ultimate goal is to achieve high capacity while satisfying quality of Service (QoS) requirements. An architecture that will easily accommodate system growth must also be implemented.

Microcells are a straight forward solution for achieving high capacity. However, as microcells are introduced, a mixed cell architecture naturally evolves, consisting of overlaid macrocells and underlaid microcells. We call such an arrangement a hierarchical architecture. Hierarchical architectures can be implemented for TDMA, CDMA, and OFDMA cellular systems. When microcells are introduced a key issue is the partitioning of the frequency resources among the hierarchical layers. The most attractive hierarchical systems are those that do not partition the system bandwidth among the hierarchical layers. If the entire bandwidth is used in each hierarchical layer, then both high capacity and high flexibility will be achieved. CDMA systems use universal frequency reuse, but require sophisticated power control algorithms if the bandwidth is not partitioned between the hierarchical layers.

Macrodiversity architectures are another method for achieving high capacity, where the signal transmitted by a mobile station (MS) is received by multiple base stations (BSs). Likewise, the signal that is received by an MS may be transmitted by multiple BSs. Macrodiversity is an effective method for combatting shadow and envelope fading. In fact, cellular handoff algorithms implement a form of macrodiversity. The soft handoff techniques used in CDMA systems are a well-known method for realizing macrodiversity. TDMA systems that use hard handoff algorithms will not yield as much macrodiversity gain due to latencies in the hard handoff algorithms. The requirement for hard handoff in TDMA systems arises a result of frequency planning with fixed channel assignment (FCA). However, if

G.L. Stüber, *Principles of Mobile Communication*, DOI 10.1007/978-1-4614-0364-7_11, 621

dynamic channel assignment (DCA) techniques are used, then TDMA systems can realize benefits from soft handoff similar to those obtained in CDMA systems. DCA techniques do not permanently assign channels to cells.

The remainder of this chapter begins with a discussion of basic cellular frequency planning techniques, including cell sectoring in Sect. 11.1 and cell splitting and reuse partitioning in Sect. 11.2. Afterwards, Sect. 11.3 considers issues related to frequency planning in OFDMA/SC-FDMA cellular networks. Section 11.4 considers a novel TDMA hierarchical cellular architecture based on the concept of cluster planning, where macrocells and microcells can share the same frequencies. Finally, Sect. 11.5 considers macrodiversity TDMA architectures, where a mobile station is simultaneously served by multiple base stations.

11.1 Cell Sectoring

11.1.1 Cell Sectoring with Wide-beam Directional Antennas

One of the simplest and most practical methods for controlling co-channel interference (CCI) is to use wide-beam directional antennas at the BSs. On the forward channel, wide-beam directional antennas reduce the generation of CCI by transmitting the signals to the MSs with a narrower angle-of-departure (AoD) spread than omnidirectional antennas. On the reverse channel, wide-beam directional antennas reduce the effect of the CCI because they respond to CCI that is received within a narrower angle-of-arrival (AoA) spread about the target MS than would be the case with omnidirectional antennas.

Consider a uniform deployment of hexagonal cells, where the BSs use omnidirectional antennas. Suppose that we ignore the effects of shadowing and multipath-fading, and assume the following simple path loss model adapted from (2.326), such that the received area mean power at distance d is

$$\mu_{\Omega_p} = \Omega_t G_T G_R \frac{(h_b h_m)^2}{d^\beta}, \tag{11.1}$$

where Ω_t is the transmit power, G_T and G_R are the transmit and receiver antenna gains, respectively, and h_b and h_m are the heights of the BS and MS antennas, respectively. As illustrated in Fig. 11.1, the worst case forward channel CCI situation occurs when the MS is located at the corner of a cell, furthest from its serving BS. For $N = 7$, there are six first-tier co-channel BSs, located at distances $\{\sqrt{13}R, 4R, \sqrt{19}R, 5R, \sqrt{28}R, \sqrt{31}R\}$ from the MS. If the values of Ω_t, G_T, and h_b are assumed to be the same for all BS antennas, then it follows that the worst case carrier-to-interference ratio, Λ, is

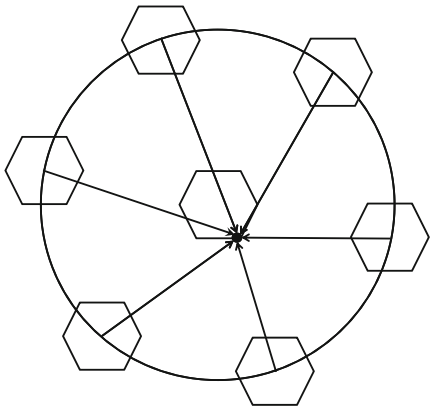

Fig. 11.1 Worst case CCI situation on the forward channel

$$\Lambda = \frac{R^{-\beta}}{(\sqrt{13}R)^{-\beta} + (4R)^{-\beta} + (\sqrt{19}R)^{-\beta} + (5R)^{-\beta} + (\sqrt{28}R)^{-\beta} + (\sqrt{31}R)^{-\beta}}$$
$$= \frac{1}{(\sqrt{13})^{-\beta} + (4)^{-\beta} + (\sqrt{19})^{-\beta} + (5)^{-\beta} + (\sqrt{28})^{-\beta} + (\sqrt{31})^{-\beta}}. \quad (11.2)$$

A similar expression can be derived for the case of $N = 3$ with co-channel distances $\{2R, \sqrt{7}R, \sqrt{7}R, \sqrt{13}R, \sqrt{13}R, 4R\}$, and $N = 4$ with co-channel distances $\{\sqrt{7}R, \sqrt{7}R, \sqrt{13}R, \sqrt{13}R, \sqrt{19}R, \sqrt{19}R\}$. With a path loss exponent $\beta = 3.5$, the worst case Λ is

$$\Lambda_{(\text{dB})} = \begin{cases} 14.56 \text{ dB} & \text{for } N = 7, \\ 9.98 \text{ dB} & \text{for } N = 4, \\ 7.33 \text{ dB} & \text{for } N = 3. \end{cases}$$

The minimum allowable cluster size is determined by the threshold carrier-to-interference ratio requirement, Λ_{th}, of the radio receiver. Unfortunately, the above worst case Λ values may be too small to yield acceptable performance, especially when we account for shadowing and multipath-fading.

Sectoring is a very common method that is used in cellular systems to improve the worst case Λ, whereby the cells are divided into radial sectors with wide-beam directional BS antennas. Cellular systems are quite often deployed with 120° and sometimes 60° cell sectors. An N-cell reuse cluster with 120° sectors yields an $N/3N$ reuse plan (N cells and $3N$ sectors). As shown in Fig. 11.2, 120° cell sectoring reduces the number of first-tier co-channel interferers from six to two. For $N = 7$, the two first-tier interferers are located at distances $\sqrt{19}R, \sqrt{28}R$ from the MS. The resulting worst case carrier-to-interference ratio, Λ, is

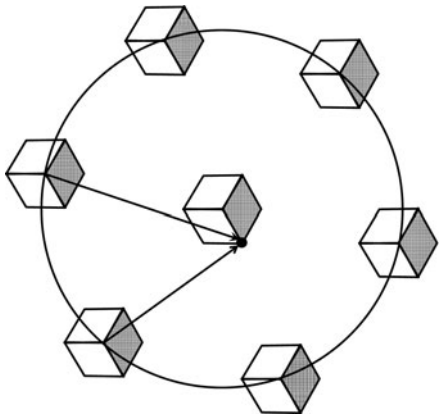

Fig. 11.2 Worst case CCI situation on the forward channel with 120° cell sectoring

$$\Lambda = \frac{R^{-\beta}}{(\sqrt{19}R)^{-\beta} + (\sqrt{28}R)^{-\beta}}$$
$$= \frac{1}{(\sqrt{19})^{-\beta} + (\sqrt{28})^{-\beta}}. \tag{11.3}$$

A similar expression can be derived for the case of $N = 3$ with co-channel distances $\{\sqrt{7}R, \sqrt{13}R$, and $N = 4$ with co-channel distances $\{\sqrt{13}R, \sqrt{19}R\}$. Hence,

$$\Lambda_{(\mathrm{dB})} = \begin{cases} 20.60\,\mathrm{dB} & \text{for } N = 7, \\ 17.69\,\mathrm{dB} & \text{for } N = 4, \\ 13.52\,\mathrm{dB} & \text{for } N = 3. \end{cases}$$

For $N = 7$, 120° sectoring yields a 6.04 dB gain in the worst case Λ over the case when omnidirectional antennas are used.

To derive a benefit from sectoring, the channel set that is assigned to each cell must be further partitioned into disjoint sets, such that each sector uses a disjoint set of channels. This finer partitioning of the channel sets results in a loss in trunking efficiency, as discussed in Sect. 1.7.3. Hence, cell sectoring improves the worst case carrier-to-interference ratio performance at the cost of reduced trunking efficiency.

11.2 Conventional Cell Splitting

Conventional cell splitting is a straight forward process of introducing new, smaller, cells into an existing cellular deployment. By doing so, the cellular system can be tailored to meet traffic growth. To illustrate conventional cell splitting, consider

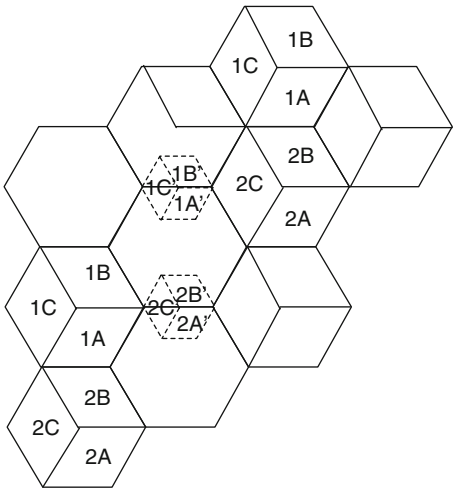

Fig. 11.3 Conventional cell splitting is used to accommodate an increased traffic load by introducing smaller cells

the uniform grid of hexagonal cells shown in Fig. 11.3. If heavy traffic loading is experienced at the midpoint between the two cells labeled **1**, then a split cell labeled **1'** is introduced at that location. The area of the split cell is 1/4 of the area of the parent cells. Additional split cells can be introduced to accommodate traffic loading in other locations throughout the system area. For example, the split cell labeled **2'** can be located at the midpoint between the two cells labeled **2**.

Because the split cells are smaller, the transmit power can be reduced. To estimate the transmit power requirements in the split cells, assume the simple path loss model in (1.5). Then the received power for an MS located at the corner of a parent cell is

$$\Omega(R_{\mathrm{o}}) = k\Omega_{\mathrm{o}}R_{\mathrm{o}}^{-\beta}, \tag{11.4}$$

while the received power at the boundary of a split cell is

$$\Omega(R_{\mathrm{s}}) = k\Omega_{\mathrm{s}}R_{\mathrm{s}}^{-\beta}. \tag{11.5}$$

where Ω_{o} and Ω_{s}, and R_{o} and R_{s}, are the transmit power and cell radius associated with the parent cells and split cells, respectively, and k is a constant. To keep the received signal power that is associated with an MS located on the cell boundary at a constant value, the transmit power requirements of the split cell and parent cell are related as follows:

$$\Omega_{\mathrm{s}} = \Omega_{\mathrm{o}}\left(\frac{R_{\mathrm{s}}}{R_{\mathrm{o}}}\right)^{-\beta}. \tag{11.6}$$

If $\beta = 4$, then $\Omega_{\mathrm{s}} = \Omega_{\mathrm{o}}/16$, since $R_{\mathrm{s}} = R_{\mathrm{o}}/2$. Hence, the split cells can reduce their transmit power levels by 12 dB.

After introducing the split cells, changes in the frequency plan are required to avoid violations of the reuse constraint. A very straight forward approach is

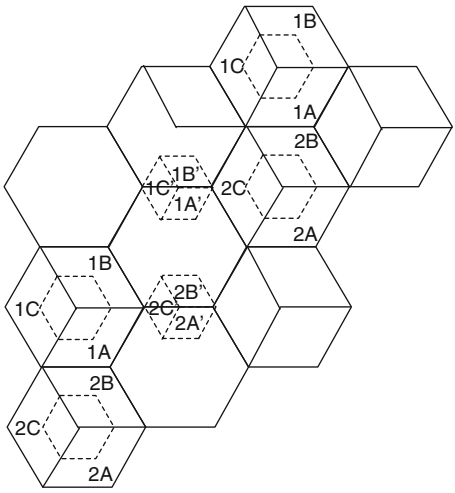

Fig. 11.4 Overlaid inner cells can be used to maintain the frequency reuse constraint when cell splitting is used

channel segmenting, where the channel sets in the co-channel cells are divided into two groups: the split cells are assigned one group of channels, while the parent co-channel cells are assigned the other group of channels. Unfortunately, this arrangement sacrifices trunking efficiency because the parent cells cannot use the channels assigned to the split cells. Furthermore, if the parent cells are already near capacity, then segmentation of the channels in these cells will require the introduction of more split cells. Hence, a propagation of cell splitting occurs throughout the system area, requiring the installation of a large number of additional cell sites. Therefore, channel segmenting may not always be a good option.

Another solution is shown in Fig. 11.4, where overlaid inner cells are introduced into the parent cells. Once again, the channels sets are divided into two groups. MSs located within the overlaid inner cells and the split cells use one group of channels, while MSs located within the outer cells use the other group of channels. Whenever an MS moves between the inner and outer areas of a cell a hand-off must be executed, to avoid violations of the co-channel reuse constraint.

11.2.1 Reuse Partitioning

Halpern [125] suggested an overlay/underlay scheme based on the concept of reuse partitioning, where multiple co-channel reuse factors are used in the same deployment. Sometimes this is called fractional reuse. An inner cell is created within each of the existing cells as shown in Fig. 11.5. For the example in Fig. 11.5, channels are assigned to the inner and outer cells according to a 3-cell and 7-cell reuse plan, respectively, although other reuse plans could be used. Channels that are assigned to the inner and outer cells can only be used by MSs located within the

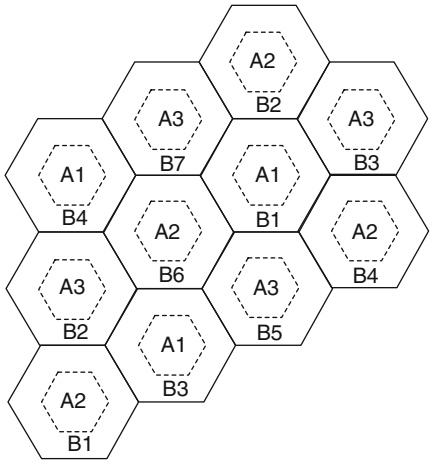

Fig. 11.5 Reuse partitioning can be used to increase the channel reuse efficiency, from [125]

inner and outer cells, respectively. Handoffs are required when an MS crosses the boundary between an inner and outer cell. The reduced radii of the inner cells lead to an increase in cell capacity. To quantify this increase let

$$R_{\mathrm{i}} = \text{radius of the inner cells.}$$

$$R_{\mathrm{o}} = \text{radius of the outer cells.}$$

$$D_{\mathrm{i}} = \text{reuse distance for the inner cells.}$$

$$D_{\mathrm{o}} = \text{reuse distance for the outer cells.}$$

Suppose that an acceptable link quality requires a co-channel reuse factor $D_{\mathrm{i}}/R_{\mathrm{i}} = D_{\mathrm{o}}/R_{\mathrm{o}} = 4.6$. If a 7-cell and 3-cell reuse cluster is used for the outer and inner cells, respectively, then $D_{\mathrm{i}}/R_{\mathrm{o}} = 3$ and

$$\frac{D_{\mathrm{i}}/R_{\mathrm{i}}}{D_{\mathrm{i}}/R_{\mathrm{o}}} = \frac{4.6}{3}. \tag{11.7}$$

Hence, the inner and outer cell radii are related by $R_{\mathrm{i}} = 0.65R_{\mathrm{o}}$ and, therefore, the inner and outer cell areas are related by $A_{\mathrm{i}} = (0.65)^2 A_{\mathrm{o}} = 0.43A_{\mathrm{o}}$. If a total of N_{T} channels are available, then $0.43N_{\mathrm{T}}$ channels should be assigned to the inner cells and $0.57N_{\mathrm{T}}$ channels assigned to the outer cell area (assuming a homogenous traffic distribution throughout the system area). The resulting cell capacity is

$$N_{\mu} = 0.57N_{\mathrm{T}}/7 + 0.43N_{\mathrm{T}}/3 = 0.225N_{\mathrm{T}} \text{ channels/cell.} \tag{11.8}$$

On the other hand, with a conventional 7-cell reuse plan

$$N_{\mu} = N_{\mathrm{T}}/7 \text{ channels/cell.} \tag{11.9}$$

Hence, an improvement of 1.575 in cell capacity is realized.

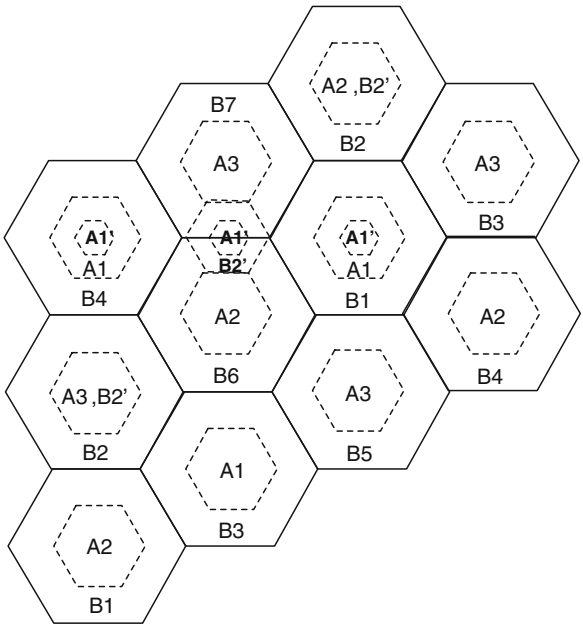

Fig. 11.6 Cell splitting can be used in combination with reuse partitioning

11.2.1.1 Cell Splitting with Reuse Partitioning

Cell splitting can also be used with reuse partitioning. An example is shown in Fig. 11.6 where a split cell is added between the parent cells labeled **B2**. The split cell also uses reuse partitioning. To maintain the C/I at an acceptable level, some of the channels in the **B2** cells are moved to the inner cells and are denoted by **B2'**. Furthermore, the closest co-channel inner cells **A1** must have their channels partitioned in a similar fashion. Thus, we see a drawback when cell splitting is used with the reuse partitioning, in that the cells must be divided into many concentric rings that use disjoint channel sets and handoffs must occur when an MS crosses the boundary between such rings.

11.3 OFDMA Radio Planning

Radio planning for OFDMA/SC-FDMA networks is more akin to radio planning in TDMA cellular networks, such as GSM, than radio planning in CDMA networks, such as WCDMA and cdma2000. The reason is that the intra-cell interference is essentially eliminated due to the orthogonal property of the OFDMA sub-carriers. However, to achieve high capacity with OFDMA/SC-FDMA networks, aggressive frequency planning is necessary, and this will tend to increase the level of inter-cell interference. For OFDMA/SC-FDMA networks adjacent channel

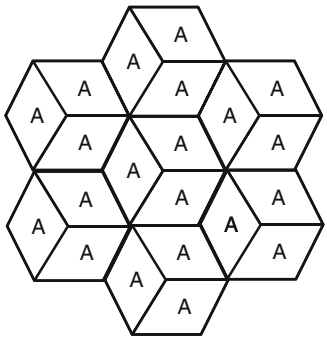

Fig. 11.7 Deployment with a sector reuse factor of 1

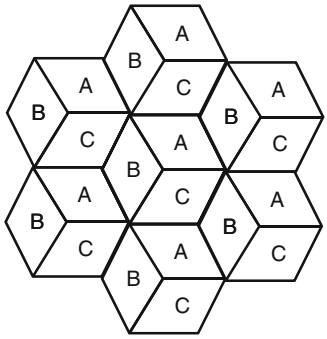

Fig. 11.8 Deployment with a sector reuse factor of 3

interference is controlled by the orthogonal nature of the sub-carriers. However, co-channel interference will be present. The reuse partitioning schemes discussed in Sect. 11.2.1 can be used for deployment, along with the cell spitting techniques in Sect. 11.2.1.1. The frequency reuse configurations that are of most interest for OFDMA/SC-FDMA networks are BSs with 120^{o} sectoring, and a sector reuse of 1 or 3.

With a sector reuse of 1, also known as universal frequency reuse, all sectors can use the same sub-carrier frequencies, as shown in Fig. 11.7. With universal frequency reuse, two different schemes can be used to mitigate the co-channel interference between the cells and along the sector boundaries, namely interference avoidance and interference randomization. Interference avoidance assigns sets of sub-carriers dynamically so as to avoid interference. Randomization can be achieved by scrambling the set of sub-carriers that are used within the same band, or by frequency hopping over a larger band. In either case, the interference experienced by the users is randomized and a strong interferer is shared by all the users.

With a sector reuse of three, the three reuse sectors in each cell are assigned a disjoint set of sub-carrier frequencies, as shown in Fig. 11.8. Reuse three will eliminate the co-channel interference that occurs along the sector boundaries in the same cell. Furthermore, it also increases the co-channel reuse distance. This will permit greater usage of the sub-carrier frequencies in each sector which will improve

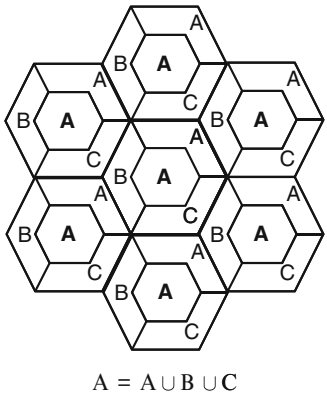

Fig. 11.9 Deployment with reuse partitioning

spectral efficiency. However, a sector reuse of three does require that the set of frequencies be partitioned into three groups which will tend to decrease spectral efficiency.

A third alternative is to use the concept of reuse partitioning as detailed in Sect. 11.2.1. With reuse partitioning a cell is divided into multiple regions, for example, an inner cell and three outer cell sectors as shown in Fig. 11.9. Users that are located in the inner cells can reuse all the available sub-carrier frequencies. Users that are located in the outer cell areas use a fraction of the available sub-carriers according to a three-sector reuse. This arrangement will yield high spectral efficiency using all the available sub-carrier frequencies in the inner cells, while at the same time provide robustness against interference using a three-sector reuse of sub-carrier frequencies in the outer cell areas. The spectral efficiency will be somewhere between that of universal frequency reuse and three-sector reuse. The scheme also requires that the locations of the users be tracked and the set of sub-carriers allocated to the users be dynamically updated according to a policy that promotes uniform sub-carrier-to-interference-plus-noise ratio (sub-carrier CIR) while maximizing a metric such as the sum capacity. For cellular downlink applications, power and sub-carrier allocation schemes can be used under the assumption that the BS has complete channel state information for all forward channels it serves, and the total BS transmit power is constrained. The uplink is similar, but more complicated in the sense that each MS may have a different transmit power constraint.

A variety of techniques described previously for single-carrier systems can be applied with simple modification to multiuser multi-carrier systems. On the forward channel beam-forming can be used to promote good spatial efficiency by minimizing BS emissions. For line-of-sight (LoS) channels, classical beam-forming is described in Sect. 6.9. In this case, it is possible that the same antenna weighting vector could be used for all sub-carriers. On the reverse channel, multi-antenna interference cancelation techniques can be performed, such as optimum combining as described in Sect. 6.8. Since the channel varies each uplink user and each sub-carrier, optimum combining would have to be used on a per user per sub-carrier basis.

11.4 Cluster-Planned Hierarchical Architecture

One drawback of conventional cell splitting and reuse partitioning is that the split cells and overlaid cells can only be introduced at specific locations in the cellular deployment. Unfortunately, these locations may not necessarily correspond to the locations that are experiencing the highest traffic growth. We now describe a TDMA hierarchical architecture based on the concept of cluster planning, where macrocells and microcells reuse the same frequencies. Moreover, the microcells can be gradually and extensively deployed at any location to increase the capacity throughout the entire service area. With these flexibilities, the cluster planning approach allows the smooth evolution of existing macrocellular systems into a hierarchical mixed cell architecture.

11.4.1 System Architecture

A traditional 7/21 frequency reuse system is shown in Fig. 11.10. The channels are partitioned into 21 sets and each set is reused in a diamond-shaped sector with an adequate distance of separation. Unfortunately. the interfering regions

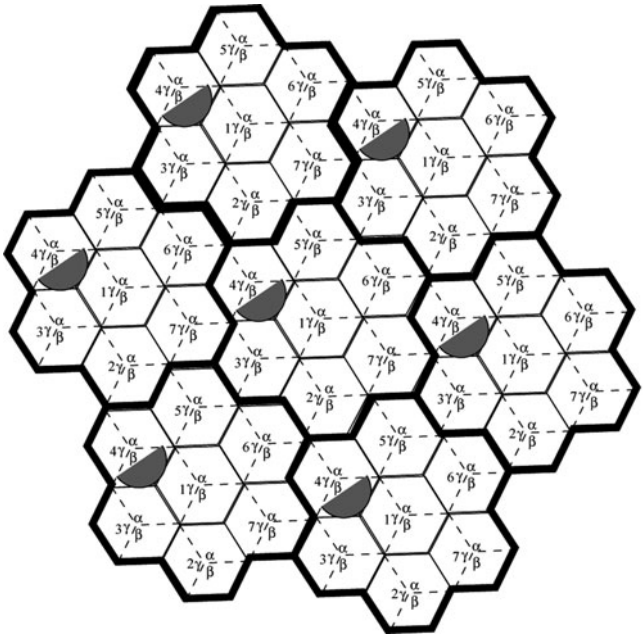

Fig. 11.10 Traditional 7/21 frequency reuse plan

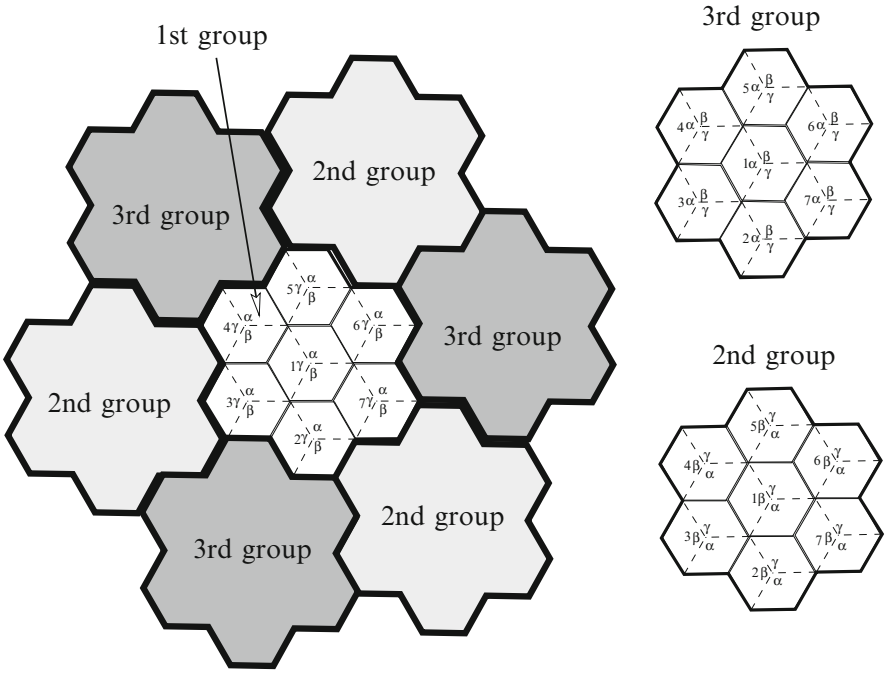

Fig. 11.11 Proposed 7/21 frequency reuse plan with cluster planning

for each channel cover the whole service area. This widely distributed CCI from the macrocells makes it impossible to reuse the same channel frequencies in the microcells.

Cluster planning can be used to change the conventional sectored arrangement into one having some areas of very low interference for a specified set of carriers. The basic cluster planning procedure is as follows:

1. Assign the same channels to each cell site as in the traditional 7/21 frequency reuse plan shown in Fig. 11.10.
2. Divide the macrocell reuse clusters into three groups as shown in Fig. 11.11.
3. Let the first group be the reference group.
4. Rotate the channel sets of each cell in the second group 120° *clockwise* with respect to the first group.
5. Rotate the channel sets of each cell in the third group 120° *counter-clockwise* with respect to the first group.

The cluster planning procedure creates low-interference regions outside the areas of the designated macrocell sectors for each channel set. These low-interference regions are called micro-areas. Fig. 11.12 shows the result of rotating the sectors. We see that zones A–F have a very low interference for channel set 4_β, since they are located in the back-lobe areas of the macrocell sectors using channel set 4_β. Thus, microcells can be introduced in these areas using channel set 4_β.

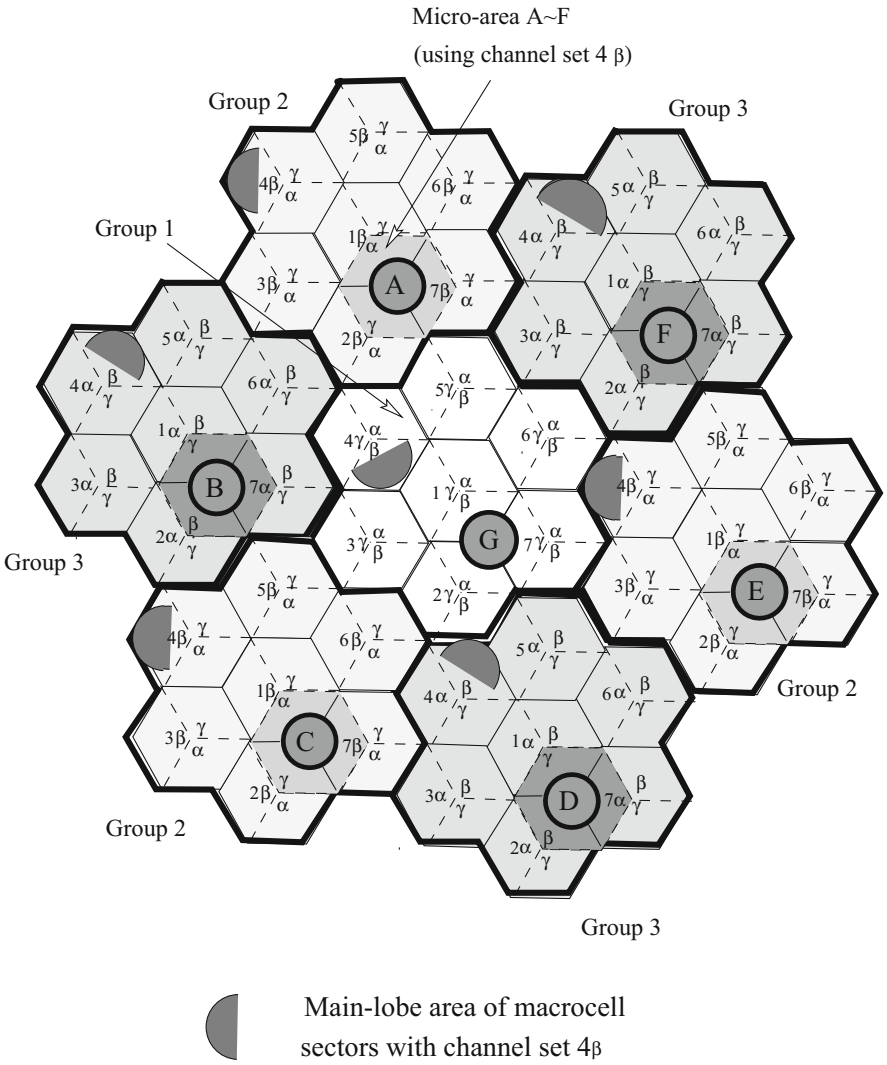

Fig. 11.12 Microcells can reuse low-interference macrocell channels in the proposed hierarchical architecture. The macrocell channel set 4_β can be reused in the micro-area A–F

11.4.2 Underlaid Microcell Planning Algorithm

In the cluster-planned hierarchical architecture, microcells are located in micro-areas where certain macrocell channel sets can be reused. To have the greatest flexibility in selecting the microcell BS locations, it is important to identify all possible micro-areas and the associated channels sets that can be used by microcells that are deployed in these areas. In the cluster-planned architecture, the front-lobe

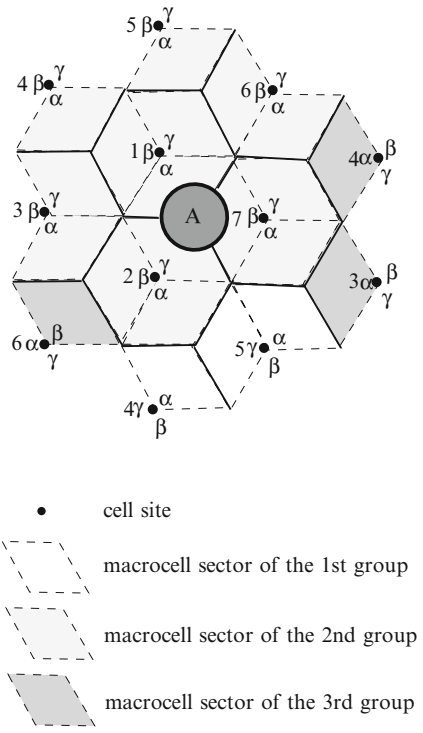

Fig. 11.13 Interference neighborhood for micro-area A in Fig. 11.12

areas of the directional antennas are used by the macrocells, while the back-lobe areas of the directional antennas are used by the microcells. In a conventional frequency reuse system (see e.g., Fig. 11.10), the back-lobe area of each channel set will still encounter some first-tier interferers. To protect the back-lobe areas from the first-tier interferers, we rotate the sectors through the cluster planning procedure. Cluster planning creates low-interference micro-areas as shown in Fig. 11.12, that lie in the back-lobe areas of the first-tier interferers. For ease of indexing, a micro-area denotes a region of three adjacent macrocell sectors, each of which belongs to different BS. Figure 11.13 shows an example of a micro-area. Each micro-area has an interference neighborhood, M, defined as the 18 neighboring macrocell sectors that surround the micro-area.

The following algorithm systematically determines the channels that can be used in each micro-area. To describe the algorithm, let c_i^j represent the channel set in sector $i = \alpha, \beta, \gamma$, of the cell site c, where $c = 1, \ldots, 7$. The superscript $j = 1, 2, 3$ indexes the three groups of rotated clusters.

- Given a desired micro-area and a corresponding interference neighborhood, M, let

$$\Theta = \left\{ c_i^j \in M \right\}$$

denote the union of channel sets c_i^j in the interference neighborhood M.

- From Θ, construct a 3×3 "indicator matrix" $\mathbf{B}_c = [b_{ij}]$ for BSs $c = 1, \ldots, 7$, where

$$b_{ij} = \begin{cases} 1 \text{ if the channel set } c_i^j \in M; \\ 0 \text{ otherwise.} \end{cases}$$

- If the indicator matrix $\mathbf{B}_c$ for some cell site c has a row of ones and two rows of zeroes, then the zero-rows of $\mathbf{B}_c$ indicate the low-interference macrocell channel sets for the micro-area.

Example 11.1:

According to Fig. 11.13, the interference neighborhood for micro-area A is

$$\Theta = \left\{1_\alpha^2, 1_\beta^2, 1_\gamma^2, 2_\alpha^2, 2_\beta^2, 2_\gamma^2, 3_\alpha^2, 3_\alpha^3, 3_\gamma^2, 4_\alpha^1, 4_\alpha^2, 4_\alpha^3, 5_\alpha^1, 5_\alpha^2, 5_\gamma^1, 6_\alpha^2, 6_\beta^2, 6_\beta^3, 7_\alpha^2, 7_\beta^2, 7_\gamma^2\right\}.$$

Then the indicating matrices are

$$\mathbf{B}_1 = \begin{pmatrix} 0\ 1\ 0 \\ 0\ 1\ 0 \\ 0\ 1\ 0 \end{pmatrix}; \quad \mathbf{B}_2 = \begin{pmatrix} 0\ 1\ 0 \\ 0\ 1\ 0 \\ 0\ 1\ 0 \end{pmatrix}; \quad \mathbf{B}_3 = \begin{pmatrix} 0\ 1\ 1 \\ 0\ 0\ 0 \\ 0\ 1\ 0 \end{pmatrix};$$

$$\mathbf{B}_4 = \begin{pmatrix} 1\ 1\ 1 \\ 0\ 0\ 0 \\ 0\ 0\ 0 \end{pmatrix}; \quad \mathbf{B}_5 = \begin{pmatrix} 1\ 1\ 0 \\ 0\ 0\ 0 \\ 1\ 0\ 0 \end{pmatrix}; \quad \mathbf{B}_6 = \begin{pmatrix} 0\ 1\ 0 \\ 0\ 1\ 1 \\ 0\ 0\ 0 \end{pmatrix};$$

$$\mathbf{B}_7 = \begin{pmatrix} 0\ 1\ 0 \\ 0\ 1\ 0 \\ 0\ 1\ 0 \end{pmatrix}.$$

Examining the indicator matrices $\mathbf{B}_c, c = 1, \ldots, 7$, we find that $\mathbf{B}_4$ is the only matrix having a row of ones and two rows of zeroes; the second and the third rows of $\mathbf{B}_4$ are the zero rows. Based on the above algorithm, the low-interference macrocell channel sets for micro-area A are 4_β and 4_γ.

To see if other micro-areas can be defined in the proposed system architecture, consider the system in Fig. 11.14 having 100 micro-areas defined over the service area. By applying the above algorithm, the available macrocell channel sets for each micro-area are listed in Table 11.1. Note that the micro-areas are capable of reusing two macrocell channel sets and microcells can be deployed throughout the whole service area.

Since a micro-area consists of three macrocell sectors, each macrocell area has five available channel sets; three are assigned to macrocells and two are assigned to microcells. Within each micro-area the microcells are deployed according to

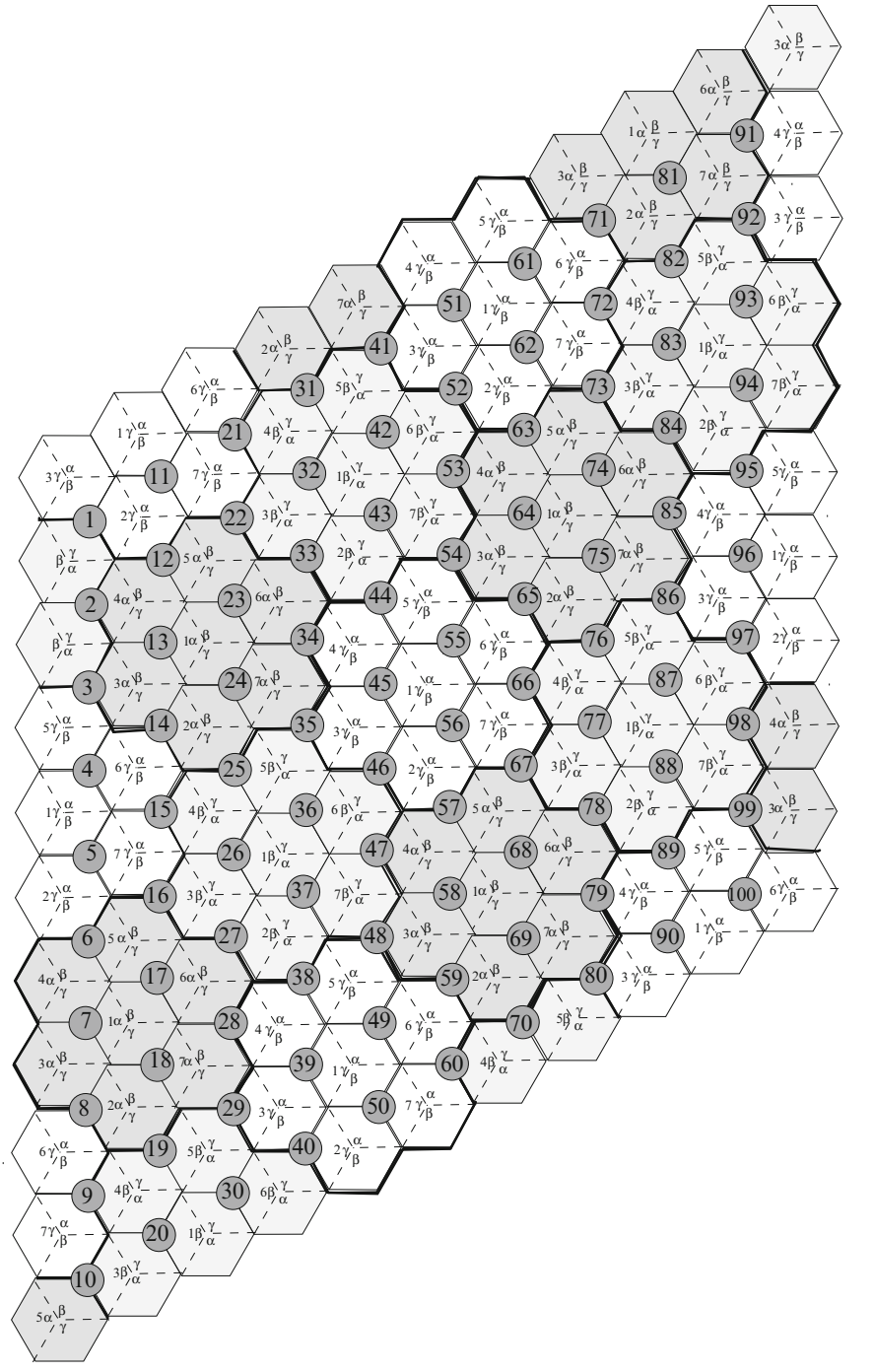

Fig. 11.14 Channel reuse in the proposed three-sector cellular system, where each micro-area consists of three sectors that belong to three different macrocells

Table 11.1 The macrocell channel sets that can be used in the underlaid microcells

Zone	*Channel set*	*Zone*	*Channel set*	*Zone*	*Channel set*	*Zone*	*Channel set*
1	$7_\alpha, 7_\beta$	26	$6_\alpha, 6_\gamma$	51	$6_\alpha, 6_\beta$	76	$3_\alpha, 3_\beta$
2	$5_\beta, 5_\gamma$	27	$7_\alpha, 7_\gamma$	52	$7_\alpha, 7_\beta$	77	$6_\alpha, 6_\gamma$
3	$1_\beta, 1_\gamma$	28	$5_\alpha, 5_\beta$	53	$5_\beta, 5_\gamma$	78	$7_\alpha, 7_\gamma$
4	$2_\beta, 2_\gamma$	29	$1_\alpha, 1_\beta$	54	$1_\beta, 1_\gamma$	79	$5_\alpha, 5_\beta$
5	$4_\alpha, 4_\gamma$	30	$2_\alpha, 2_\beta$	55	$2_\beta, 2_\gamma$	80	$1_\alpha, 1_\beta$
6	$3_\alpha, 3_\gamma$	31	$3_\alpha, 3_\beta$	56	$4_\alpha, 4_\gamma$	81	$4_\alpha, 4_\beta$
7	$6_\beta, 6_\gamma$	32	$6_\alpha, 6_\gamma$	57	$3_\alpha, 3_\gamma$	82	$3_\alpha, 3_\beta$
8	$7_\beta, 7_\gamma$	33	$7_\alpha, 7_\gamma$	58	$6_\beta, 6_\gamma$	83	$6_\alpha, 6_\gamma$
9	$5_\alpha, 5_\gamma$	34	$5_\alpha, 5_\beta$	59	$7_\beta, 7_\gamma$	84	$7_\alpha, 7_\gamma$
10	$1_\alpha, 1_\gamma$	35	$1_\alpha, 1_\beta$	60	$5_\alpha, 5_\gamma$	85	$5_\alpha, 5_\beta$
11	$4_\alpha, 4_\gamma$	36	$2_\alpha, 2_\beta$	61	$2_\beta, 2_\gamma$	86	$1_\alpha, 1_\beta$
12	$3_\alpha, 3_\gamma$	37	$4_\beta, 4_\gamma$	62	$4_\alpha, 4_\gamma$	87	$2_\alpha, 2_\beta$
13	$6_\beta, 6_\gamma$	38	$3_\beta, 3_\gamma$	63	$3_\alpha, 3_\gamma$	88	$4_\beta, 4_\gamma$
14	$7_\beta, 7_\gamma$	39	$6_\alpha, 6_\beta$	64	$6_\beta, 6_\gamma$	89	$3_\beta, 3_\gamma$
15	$5_\alpha, 5_\gamma$	40	$7_\alpha, 7_\beta$	65	$7_\beta, 7_\gamma$	90	$6_\alpha, 6_\beta$
16	$1_\alpha, 1_\gamma$	41	$1_\alpha, 1_\beta$	66	$5_\alpha, 5_\gamma$	91	$5_\alpha, 5_\beta$
17	$2_\alpha, 2_\gamma$	42	$2_\alpha, 2_\beta$	67	$1_\alpha, 1_\gamma$	92	$1_\alpha, 1_\beta$
18	$4_\alpha, 4_\beta$	43	$4_\beta, 4_\gamma$	68	$2_\alpha, 2_\gamma$	93	$2_\alpha, 2_\beta$
19	$3_\alpha, 3_\beta$	44	$3_\beta, 3_\gamma$	69	$4_\alpha, 4_\beta$	94	$4_\beta, 4_\gamma$
20	$6_\alpha, 6_\gamma$	45	$6_\alpha, 6_\beta$	70	$3_\alpha, 3_\beta$	95	$3_\beta, 3_\gamma$
21	$5_\alpha, 5_\gamma$	46	$7_\alpha, 7_\beta$	71	$7_\beta, 7_\gamma$	96	$6_\alpha, 6_\beta$
22	$1_\alpha, 1_\gamma$	47	$5_\beta, 5_\gamma$	72	$5_\alpha, 5_\beta$	97	$7_\alpha, 7_\beta$
23	$2_\alpha, 2_\gamma$	48	$1_\beta, 1_\gamma$	73	$1_\alpha, 1_\gamma$	98	$5_\beta, 5_\gamma$
24	$4_\alpha, 4_\beta$	49	$2_\beta, 2_\gamma$	74	$2_\alpha, 2_\gamma$	99	$1_\beta, 1_\gamma$
25	$3_\alpha, 3_\beta$	50	$4_\alpha, 4_\gamma$	75	$4_\alpha, 4_\beta$	100	$2_\beta, 2_\gamma$

a conventional frequency reuse plan. The microcells could use omnidirectional antennas or sectored antennas. Let C_μ represent the number of the microcell clusters that are deployed in a micro-area. Since each microcell cluster can reuse two sets of low-interference macrocell channels as shown in the above example, the cell capacity can be increased by factor of $1 + 2 \times C_\mu/3$ times. Later we will show that $C_\mu = 6$ is possible and, hence, giving a capacity increase of seven times.

11.4.3 Performance Analysis of Cluster-Planned Architecture

11.4.3.1 Propagation Model and System Assumptions

Our analysis uses the following path loss model from (2.326):

$$\mu_{\Omega_\mathrm{p}} = \frac{\Omega_\mathrm{t}(h_\mathrm{b}h_\mathrm{m})^2}{d^\beta}, \tag{11.10}$$

where μ_{Ω_p} and Ω_t are the received and transmitted powers, h_b and h_m are the BS and MS antenna heights, respectively, d is the radio path length, and β is the path

loss exponent. Although (11.10) is more suitable for a macrocell environment than a microcell environment, it is still the characteristic of the path loss experienced by the microcell links at locations that are well outside of the microcells. In other words, the model is applicable when considering the CCI that is generated by distant microcells.

CCI: In our two-tiered hierarchical architecture, four types of CCI must be considered; macrocell-to-macrocell, microcell-to-microcell, macrocell-to-microcell and microcell-to-macrocell CCI. Adjacent channel interference should also be considered.

Antennas: The macrocell BSs are assumed to use 120^{o} wide-beam directional antennas, while microcell BSs use omni-directional antennas. It is possible to improve the C/I performance by sectoring the microcells as well, but we do not consider this here. The MSs use omnidirectional antennas.

Uplink power control: We adopt an uplink power control scheme such that the transmitted power is adjusted in six levels from -22 dBW to -2 dBW in steps of 4 dB. Downlink power control is not required in the proposed architecture. Before proceeding, we first clarify our notation. When the subscripts M and μ are used, they refer to macrocells and microcells, respectively; when m and b are used, they denote the MS and BS, respectively; when d and u are used, they indicate the downlink and uplink, respectively.

11.4.3.2 Macrocell Performance

Section 11.4.2 showed that the cluster planning technique creates low interference regions, thereby allowing the microcells to reuse macrocell frequencies. However, some macrocells will experience higher interference after rotating the sectors. This is the cost of cluster planning. To evaluate the influence of the sector rotations on the macrocell performance, consider both the conventional macrocellular system in Fig. 11.10 and the proposed hierarchical cellular system in Fig. 11.12 without the underlaid microcells. Figure 11.15 shows the simulation results of the uplink C/I performance for both systems, assuming that the MSs are uniformly distributed in each sector and they transmit with the maximum power. We consider the uplink case because the downlink performance is usually better than the uplink performance. With respect to a 90% coverage probability, one can observe that the sector rotation technique creates low interference regions at the cost of about 3.1, 3.3, and 3.5 dB of C/I degradation for path loss exponent $\beta = 3.6$, 3.8, and 4.0, respectively. Even after sector rotations, the macrocells can maintain a C/I greater than 20 dB over 90% of the coverage area. In the following, we will further include the effect of

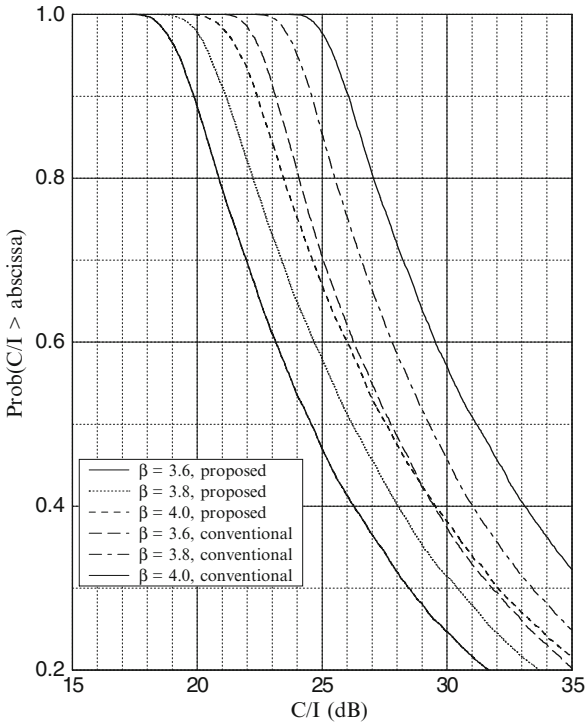

Fig. 11.15 Comparison of the uplink C/I performance of conventional macrocells and the proposed hierarchical cellular system without the underlaid microcells for different path loss exponent β

underlaid microcells when analyzing the performance of the proposed hierarchical cellular system. For ease of analysis, we hereafter adopt the worst case scenario where an MS is situated on a cell boundary.

Downlink *C/I* Analysis

By applying (11.10) with $\beta = 4$, we express the C/I received by the MS at the macrocell boundary as

$$\frac{C_{\mathrm{M}}^{\mathrm{d}}}{I_{\mathrm{M}}^{\mathrm{d}} + J_{\mu\mathrm{M}}^{\mathrm{d}}} = \frac{\Omega_{\mathrm{t,b}}^{\mathrm{M}} \dfrac{(h_{\mathrm{b}}^{\mathrm{M}} h_{\mathrm{m}})^2}{R_{\mathrm{M}}^4}}{\displaystyle\sum_{i=1}^{N_{\mathrm{M}}} \frac{\Omega_{\mathrm{t,b}}^{\mathrm{M}} (h_{\mathrm{b}}^{\mathrm{M}} h_{\mathrm{m}})^2}{D_i^4} + \sum_{j=1}^{Z_\mu} \sum_{k=1}^{C_\mu} \frac{\Omega_{\mathrm{t,b}}^{\mu} (h_{\mathrm{b}}^{\mu} h_{\mathrm{m}})^2}{{d_{jk}}^4}} \tag{11.11}$$

where

$C_{\mathrm{M}}^{\mathrm{d}}$ = MS received power from the desired macrocell BS

$I_{\mathrm{M}}^{\mathrm{d}}$ = downlink macrocell-to-macrocell CCI

$J_{\mu M}^{d}$ = downlink microcell-to-macrocell CCI

$\Omega_{t,b}^{M}$ = macrocell BS transmitted power

$\Omega_{t,b}^{\mu}$ = microcell BS transmitted power

N_M = the number of macrocell co-channel interferers

Z_μ = the number of interfering micro-areas

C_μ = the number of microcell clusters in a micro-area

D_i = MS distance to the ith interfering macrocell BS

$d_{j,k}$ = MS distance to the kth interfering microcell BS in the jth micro-area

h_b^M = macrocell BS antenna height

h_b^μ = microcell BS antenna height

h_m = MS antenna height

R_M = macrocell radius

Referring to Fig. 11.14 and Table 11.1, we examine the downlink interference when a macrocell MS using channel set 1_β is located at the macrocell boundary near micro-area 56. One can find that the macrocell-to-macrocell downlink interference I_M^d mainly comes from two first-tier macrocell BSs located near micro-areas 77 and 68 with distances $[D_1, D_2] = [4, 3.61]R_M$, respectively. However, because the objective of cluster planning is to carefully manage the C/I, the performance may be sensitive to the C/I. Consequently, we also consider the three second-tier interfering BSs located near micro-areas 11, 17, and 62, located at distances $[D_3, D_4, D_5] = [8.89, 8.89, 8.72]R_M$, respectively. For the microcell-to-macrocell downlink interference $J_{\mu M}^{d}$, one can find six interfering micro-areas 35, 48, 54, 80, 86, and 99 in the first tier with distances of $[\overline{d_1}, \overline{d_2}, \overline{d_3}, \overline{d_4}, \overline{d_5}, \overline{d_6}] = [3, 4.58, 3.46, 6, 5.2, 6.25]R_M$, respectively. The second-tier interfering micro-areas 3, 29, 41, and 92 have distances $[\overline{d_7}, \overline{d_8}, \overline{d_9}, \overline{d_{10}}] = [7.55, 9, 7.94, 12]R_M$, respectively. We assume that each micro-area has C_μ microcell reuse clusters, and each of these clusters has K_μ microcells. Through the channel selection algorithm in Sect. 11.4.2, each micro-area is assigned two macrocell channel sets. We further partition these two sets of channels into K_μ groups and then assign each group to the K_μ microcells in each cluster. In this manner, a macrocell channel set is used C_μ times in a micro-area. For ease of analysis, we assume that the distance $\overline{d_j}$ approximates $d_{j,k}$, where $\overline{d_j}$ is the distance from a macrocell MS to the center of the jth interfering micro-area and $d_{j,k}$ is defined following (11.11). In our example, the microcell BS antenna height is one-third of macrocell BS antenna height, i.e., $h_b^\mu / h_b^M = 1/3$, although this ratio can be easily varied. With the above assumptions in (11.11) we have

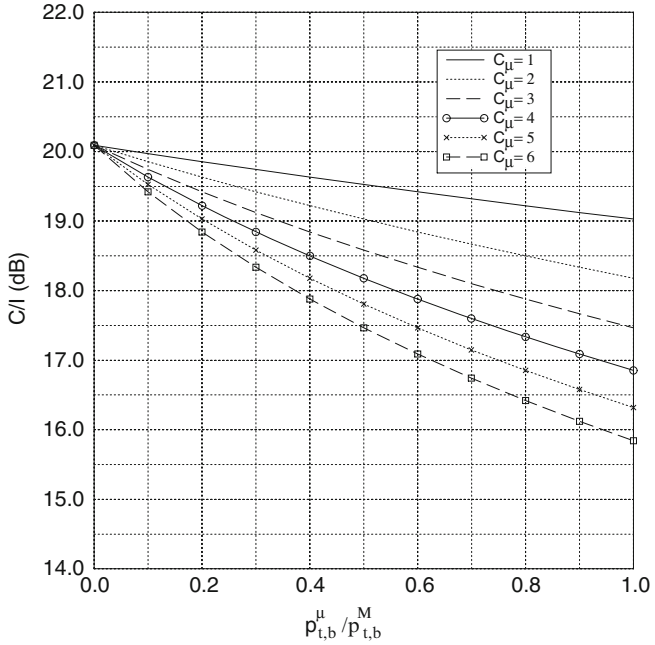

Fig. 11.16 Macrocell downlink C/I performance against $\Omega^{\mu}_{\mathrm{t,b}}/\Omega^{\mathrm{M}}_{\mathrm{t,b}}$ for different values of C_μ, where $\Omega^{\mu}_{\mathrm{t,b}}/\Omega^{\mathrm{M}}_{\mathrm{t,b}}$ is the microcell to microcell BS transmit power, and C_μ is the number of microcell clusters in a micro-area

$$\frac{C^{\mathrm{d}}_{\mathrm{M}}}{I^{\mathrm{d}}_{\mathrm{M}} + J^{\mathrm{d}}_{\mu M}} = \frac{1}{1.02875 \times 10^{-2} + C_\mu \left(\dfrac{\Omega^{\mu}_{\mathrm{t,b}}}{\Omega^{\mathrm{M}}_{\mathrm{t,b}}} \right) \times 2.79449 \times 10^{-3}}. \tag{11.12}$$

We show the downlink C/I performance in terms of C_μ and $\Omega^{\mu}_{\mathrm{t,b}}/\Omega^{\mathrm{M}}_{\mathrm{t,b}}$ in Fig. 11.16 with consideration of only first-tier interfering BSs and in Table 11.2 with both first- and second-tier interfering BSs. Observe that $\mathrm{C/I} \geq 18\,\mathrm{dB}$ for $C_\mu = 6$ and $\Omega^{\mu}_{\mathrm{t,b}}/\Omega^{\mathrm{M}}_{\mathrm{t,b}} \leq 0.3$. In other words, the channel set 4_β can be reused six times in the micro-area while still keeping the worst case macrocell downlink C/I greater than 18 dB. The reuse increases even further if the required C/I is smaller than 18 dB. Furthermore, by comparing the results in Table 11.2 with Fig. 11.16, one can find that the second-tier interfering BSs only degrade the C/I by an additional 0.5 dB over the first-tier interfering BSs.

Uplink CCI Analysis

By modifying (11.11) slightly, we can formulate the uplink C/I as

Table 11.2 Downlink C/I performance for overlaying macrocells, where $h_{\mathrm{b}}^{\mu}/h_{\mathrm{b}}^{\mathrm{M}} = 1/3$

$C_{\mathrm{M}}^{\mathrm{d}}/(I_{\mathrm{M}}^{\mathrm{d}} + J_{\mu\mathrm{M}}^{\mathrm{d}})$ (dB)				
$\Omega_{\mathrm{t,b}}^{\mu}/\Omega_{\mathrm{t,b}}^{\mathrm{M}}$	$C_{\mu} = 1$	$C_{\mu} = 2$	$C_{\mu} = 4$	$C_{\mu} = 6$
0	19.88	19.88	19.88	19.84
0.1	19.76	19.64	19.42	19.22
0.2	19.65	19.42	19.02	18.65
0.3	19.53	19.22	18.65	18.15
0.4	19.43	19.02	18.31	17.70
0.5	19.32	18.83	17.99	17.29
0.6	19.22	18.65	17.69	16.91
0.7	19.12	18.48	17.42	16.57
0.8	19.02	18.30	17.16	16.25
0.9	18.93	18.14	16.91	15.96
1.0	18.83	17.99	16.68	15.68

$$\frac{C_{\mathrm{M}}^{\mathrm{u}}}{I_{\mathrm{M}}^{\mathrm{u}} + J_{\mu\mathrm{M}}^{\mathrm{u}}} = \frac{\Omega_{\mathrm{t,m}}^{\mathrm{M}} \dfrac{(h_{\mathrm{b}}^{M} h_{\mathrm{m}})^2}{R_{\mathrm{M}}^4}}{\displaystyle\sum_{i=1}^{N_{\mathrm{M}}} \frac{\Omega_{\mathrm{t,m}}^{\mathrm{M}} (h_{\mathrm{b}}^{M} h_{\mathrm{m}})^2}{D_i^4} + \sum_{j=1}^{Z_{\mu}} \sum_{k=1}^{C_{\mu}} \frac{\Omega_{\mathrm{t,m}}^{\mu} (h_{\mathrm{b}}^{\mathrm{M}} h_{\mathrm{m}})^2}{{d_{jk}}^4}}, \tag{11.13}$$

where

$C_{\mathrm{M}}^{\mathrm{u}}$ = macrocell BS received power from the desired MS

$I_{\mathrm{M}}^{\mathrm{u}}$ = uplink macrocell-to-macrocell interference

$J_{\mu M}^{\mathrm{u}}$ = uplink microcell-to-macrocell interference

$\Omega_{\mathrm{t,m}}^{\mathrm{M}}$ = macrocell MS transmitted power

$\Omega_{\mathrm{t,m}}^{\mu}$ = microcell MS transmitted power

and where the remaining parameters have already been defined following (11.11). With directional antennas, the macrocell BSs experience fewer interfering micro-areas in the uplink direction as compared with the downlink direction. Consider the macrocell sector that is assigned with channel set 2γ and located near micro-area 37. This macrocell sector encounters two first-tier and four second-tier macrocell interfering MSs at distances

$$[D_1, D_2, D_3, D_4, D_5, D_6] = [3.61, 3.61, 8.54, 8.19, 8.19, 7.81] R_{\mathrm{m}},$$

and interfering micro-areas 23, 55, 61, 68, 74, 100, (i.e. $Z_{\mu} = 6$) at distances

$$[d_1, d_2, d_3, d_4, d_5, d_6] = [7.0, 7.0, 14.7, 5.3, 11.5, 9.53] R_{\mathrm{m}}.$$

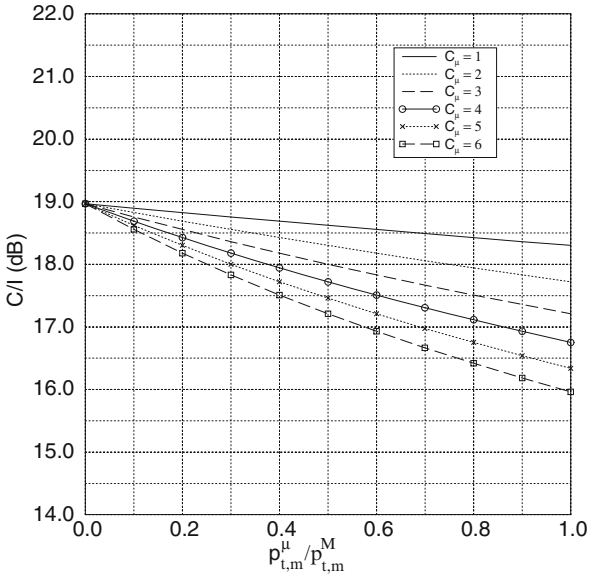

Fig. 11.17 Macrocell uplink C/I performance against $\Omega^{\mu}_{t,m}/\Omega^{M}_{t,m}$ for different values of C_{μ}, where $\Omega^{\mu}_{t,m}/\Omega^{M}_{t,m}$ is the ratio of the transmitted power of the microcell MS to that of the macrocell MS, and C_{μ} is the number of microcell clusters in a micro-area

We can ignore the effect of the three other interfering micro-areas 4, 17, 49 because they are located in the back-lobe area of the sector using channel set 2γ. By substituting the above values into (11.13), the uplink C/I performance for this example becomes

$$\frac{C^{u}_{M}}{I^{u}_{M} + J^{u}_{\mu M}} = \frac{1}{1.2677 \times 10^{-2} + C_{\mu}\left(\dfrac{\Omega^{\mu}_{t,m}}{\Omega^{M}_{t,m}}\right) \times 2.11 \times 10^{-3}}. \tag{11.14}$$

Figure 11.17 shows the results. Suppose that a worst case target C/I of 18 dB is chosen. Then it is observed that the C/I is greater than 18 dB for $C_{\mu} = 1$–6 if

$$\frac{\Omega^{\mu}_{t,m}}{\Omega^{M}_{t,m}} \leq 0.2. \tag{11.15}$$

Note that we obtained (11.15) under the assumption that the interfering macrocell MSs are on the cell boundary and are transmitting with the maximum power. Thus (11.15) can be used to determine the maximum microcell MS's transmitted power. For example, consider an MS that can adjust its transmitted power in six levels from -22 dBW to -2 dBW. Then (11.15) implies that the maximum microcell MS transmitted power is -9 dBW, which is still in the operational range of the MS.

11.4.3.3 Microcell Performance

We now show how the microcell size should be chosen to achieve the required C/I performance.

Downlink microcell size

A feasible microcell size should satisfy two conditions: (1) C-criterion: an MS will receive stronger power, C, at the microcell boundary than at the macrocell boundary; (2) C/I-criterion: the C/I at the microcell boundary equals or exceeds that at the macrocell boundary.

C-criterion: From the path loss model in (11.10), the microcell radius R_μ can be calculated as

$$R_\mu \leq \left(\left(\frac{\Omega_{\mathrm{t,b}}^{\mu}}{\Omega_{\mathrm{t,b}}^{\mathrm{M}}} \right) \left(\frac{h_{\mathrm{b}}^{\mu}}{h_{\mathrm{b}}^{\mathrm{M}}} \right)^2 \right)^{1/4} R_{\mathrm{M}}, \tag{11.16}$$

where R_{M}, h_{b}^{μ}, $h_{\mathrm{b}}^{\mathrm{M}}$, $\Omega_{\mathrm{t,b}}^{\mu}$, and $\Omega_{\mathrm{t,b}}^{\mathrm{M}}$ are defined in (11.11).

C/I-criterion: The C/I received by the MS at the microcell boundary can be written as

$$\frac{C_\mu^{\mathrm{d}}}{I_\mu^{\mathrm{d}} + J_{\mathrm{M}\mu}^{\mathrm{d}}} = \frac{\Omega_{\mathrm{t,b}}^{\mu} \dfrac{(h_{\mu,\mathrm{b}} h_{\mathrm{m}})^2}{R_\mu^4}}{\displaystyle\sum_{i=1}^{C_\mu - 1} \frac{\Omega_{\mathrm{t,b}}^{\mu} (h_{\mu,\mathrm{b}} h_{\mathrm{m}})^2}{D_{\mu_i}^4} + \sum_{i=1}^{N_{\mathrm{M}_f}} \frac{\Omega_{\mathrm{t,b}}^{M} (h_{\mathrm{M,b}} h_{\mathrm{m}})^2}{D_{\mathrm{M}_{f,i}}^4} + \frac{1}{\eta} \left(\sum_{i=1}^{N_{\mathrm{M_b}}} \frac{\Omega_{t,b}^{M} (h_{\mathrm{M,b}} h_{\mathrm{m}})^2}{D_{\mathrm{M_{b,}}i}^4} \right)}, \tag{11.17}$$

where the parameters $\Omega_{\mathrm{t,b}}^{\mu}$, $\Omega_{\mathrm{t,b}}^{\mathrm{M}}$, $h_{\mathrm{b}}^{\mathrm{M}}$, h_{b}^{μ}, C_μ, and h_{m} have already been defined in (11.11) and

C_μ^{d} = MS received power from its desired microcell BS

I_μ^{d} = downlink microcell-to-microcell interference

$J_{\mathrm{M}\mu}^{\mathrm{d}}$ = downlink macrocell-to-microcell interference

N_{Mf} = the number of main-lobe macrocell interferers

N_{Mb} = the number of back-lobe macrocell interferers

$D_{\mathrm{Mf},i}$ = MS distance to the ith main-lobe interfering BS

$D_{\mathrm{Mb},j}$ = MS distance to the jth back-lobe interfering BS

$D_{\mu,i}$ = MS distance to the ith microcell interfering BS

R_{M} = macrocell radius

R_{μ} = microcell radius

η = the front-to-back ratio of the directional antenna in macrocells

Let $(C/I)_{\mathrm{req}}$ denote the required C/I. Then (11.17) becomes

$$\frac{R_{\mu}}{R_{\mathrm{M}}} \leq \left(\frac{(C/I)_{\mathrm{req}}^{-1}}{\sum_{i=1}^{C_{\mu}-1} \left(\frac{1}{\widehat{D_{\mu_i}}} \right)^4 + \left(\sum_{i=1}^{N_{\mathrm{M_f}}} \left(\frac{1}{\widehat{D_{\mathrm{M_{f},}i}}} \right)^4 + \frac{1}{\eta} \sum_{j=1}^{N_{\mathrm{M_b}}} \left(\frac{1}{\widehat{D_{\mathrm{M_{b},}j}}} \right)^4 \right) \left(\frac{\Omega_{\mathrm{t,b}}^{\mathrm{M}}}{\Omega_{\mathrm{t,b}}^{\mu}} \right) \left(\frac{h_{\mathrm{M,b}}}{h_{\mu,\mathrm{b}}} \right)^2} \right)^{\frac{1}{4}}, \tag{11.18}$$

where $\widehat{D_{\mathrm{M_{f},}i}} = D_{\mathrm{M_{f},}i}/R_{\mathrm{M}}$, $\widehat{D_{\mathrm{M_{b},}j}} = D_{\mathrm{M_{b},}j}/R_{\mathrm{M}}$, and $\widehat{D_{\mu_i}} = D_{\mu_i}/R_{\mathrm{M}}$, are the normalized distances of interferers with respect to macrocell radius R_{M}. Here, we assume that the microcells and macrocells have similar shapes, and that the microcell clusters are adjacent to each other in a given micro-area. Suppose the distances from a microcell MS to its interfering microcell BSs are equal and close to the microcell co-channel reuse distance D_{μ} (i.e., $D_{\mu,i} = D_{\mu}$, for $i = 1, \cdots, C_{\mu}$). Then

$$\frac{D_{\mu}}{R_{\mu}} = \sqrt{3K_{\mu}}, \tag{11.19}$$

where K_{μ} denotes the microcell cluster size. With C_{μ} microcell clusters and K_{μ} microcells inside each cluster, a micro-area has in total $C_{\mu}K_{\mu}$ microcells. Suppose that taken together they are smaller than the area of a macrocell. Then

$$\frac{R_{\mathrm{M}}}{R_{\mu}} \geq \sqrt{C_{\mu}K_{\mu}}. \tag{11.20}$$

Substituting (11.19) (11.20) into (11.18), we get

$$\frac{R_{\mu}}{R_{\mathrm{M}}} \leq \left(\frac{(C/I)_{\mathrm{req}}^{-1}}{\frac{(C_{\mu}-1)C_{\mu}^2}{9} + \left(\sum_{i=1}^{N_{\mathrm{M}_f}} \left(\frac{1}{\widehat{D_{\mathrm{M}_{f,}i}}} \right)^4 + \frac{1}{\eta} \sum_{j=1}^{N_{\mathrm{M}_b}} \left(\frac{1}{\widehat{D_{\mathrm{M}_{b,}j}}} \right)^4 \right) \left(\frac{\Omega_{\mathrm{t,b}}^{M}}{\Omega_{t,b}^{\mu}} \right) \left(\frac{h_b^M}{h_b^{\mu}} \right)^2} \right)^{\frac{1}{4}}, \tag{11.21}$$

Notice that we consider N_{M_b} back-lobe macrocell interferers in (11.21). The back-lobe interference from the macrocell BSs can be ignored for the macrocell MS, but

for the microcell MS, this kind of interference may be relatively strong compared to the received signal strength from the "low-powered" microcell BS. For the same reason, the macrocell interferers in the second ring are considered here.

Example 11.2:

Referring to Fig. 11.14 and Table 11.1, micro-area 56 can be assigned channel sets $[4_\alpha, 4_\gamma]$. Take channel set 4_γ as an example. Micro-area 56 will experience three first-tier back-lobe interferers ($N_{\mathrm{M_b}} = 3$), each of which has the following distance:

$$[\widehat{D_{\mathrm{M_{b]},1}}}, \widehat{D_{\mathrm{M_{b,2}}}}, \widehat{D_{\mathrm{M_{b,3}}}}] = [2.65, 2.65, 2.65] \tag{11.22}$$

to the center of micro-area 56. Three main-lobe interfering macrocells in the second tier are located near micro-areas 25, 79, 64 with the distances of

$$\left[\widehat{D_{\mathrm{M}_{f,1}}}, \widehat{D_{\mathrm{M}_{f,2}}}, \widehat{D_{\mathrm{M}_{f,3}}}\right] = [5.29, 5.29, 5.29]. \tag{11.23}$$

Furthermore, three main-lobe interfering macrocell BSs in the third tier are located near micro-areas 13, 70, and 85 with distances of

$$\left[\widehat{D_{\mathrm{M}_{f,4}}}, \widehat{D_{\mathrm{M}_{f,5}}}, \widehat{D_{\mathrm{M}_{f,6}}}\right] = [7.0, 7.0, 7.0]. \tag{11.24}$$

It is also important to determine if there exist interfering microcell BSs from neighboring micro-areas. Figure 11.14 and Table 11.1 shows one feature of the proposed system architecture; the adjacent micro-areas are assigned different macrocell channel sets. For instance, micro-area 56 in Fig. 11.14 is assigned channel sets $[4_\alpha, 4_\gamma]$, while the neighboring micro-areas 45, 46, 55, 57, 66, and 67 use channel sets $[6_\alpha, 6_\beta]$, $[7_\alpha, 7_\beta]$, $[2_\beta, 2_\gamma]$, $[3_\alpha, 3_\gamma]$, $[5_\alpha, 5_\gamma]$, $[1_\alpha, 1_\gamma]$. Obviously, when considering the interfering microcell BSs, a microcell MS will only be affected by the interfering microcell BSs in the same micro-area. Assume that each micro-area consists of C_μ microcell clusters. Then an MS will experience the interference from the remaining $C_\mu - 1$ microcell BSs, excluding the desired one. Substituting (11.22), (11.23), and (11.24) into (11.21), one can obtain

$$\frac{R_\mu}{R_M} \leq \left(\frac{(C/I)_{\mathrm{req}}^{-1}}{\frac{(C_\mu - 1)C_\mu^2}{9} + \left(5.0803 \times 10^{-3} + 0.0608 \times \frac{1}{\eta}\right)\left(\frac{\Omega_{\mathrm{t,b}}^{\mathrm{M}}}{\Omega_{\mathrm{t,b}}^{\mu}}\right)\left(\frac{h_{\mathrm{b}}^{\mathrm{M}}}{h_{\mathrm{b}}^{\mu}}\right)^2} \right)^{\frac{1}{4}}. \tag{11.25}$$

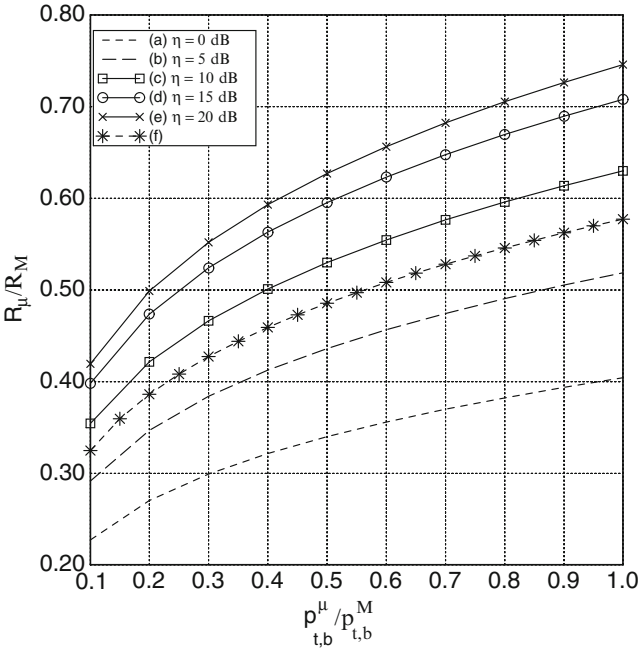

Fig. 11.18 Effect of front-to-back ratio η on the microcell radius based on downlink microcell C/I performance analysis, where $R_\mu/R_{\rm M}$ and $\Omega^{\mu}_{\rm t,b}/\Omega^{\rm M}_{\rm t,b}$ are the cell radius ratio and transmitted power ratio of microcells over macrocells, respectively. With $(C/I)_{\rm req} = 18\,{\rm dB}$ and $h^{\mu}_{\rm b}/h^{\rm M}_{\rm b} = 1/3$, curves (a)–(e) are obtained by C/I-criterion for $\eta = 0, 5, 10, 15$, and $20\,{\rm dB}$, respectively, while curve (f) is obtained by C-criterion

(a) $C_\mu = 1$**:** We first consider the special case where only one microcell is installed in each micro-area. This situation may occur with initial microcell deployment. Figure 11.18 shows the effect of the front-to-back ratio η on the microcell radius, in the case $(C/I)_{\rm req} = 18\,{\rm dB}$ and $h^{\mu}_{\rm b}/h^{\rm M}_{\rm b} = 1/3$. If the C/I- and C-criterion result in different microcell radii, then the smallest one must be chosen. From Fig. 11.18, one can observe that if front-to-back ratio $\eta \geq 10\,{\rm dB}$, the microcell radius is determined by the C-criterion, but when $\eta \leq 5\,{\rm dB}$, the C/I-criterion dominates the C-criterion. For instance, in the case of $\eta = 10\,{\rm dB}$ and $\Omega^{\mu}_{t,b}/\Omega^{M}_{t,b} = 0.4$, one can obtain $R_\mu \leq 0.5R_{\rm M}$ by the C/I-criterion and $R_\mu \leq 0.46R_{\rm M}$ by the C-criterion, respectively. We must satisfy the more stringent requirement and, therefore, the microcell radius is $0.46R_{\rm M}$. In this example, one can see that a larger front-to-back ratio η does not imply a larger microcell size, since the C-criterion, which is independent of η, will dominate the C/I-criterion when η is large.

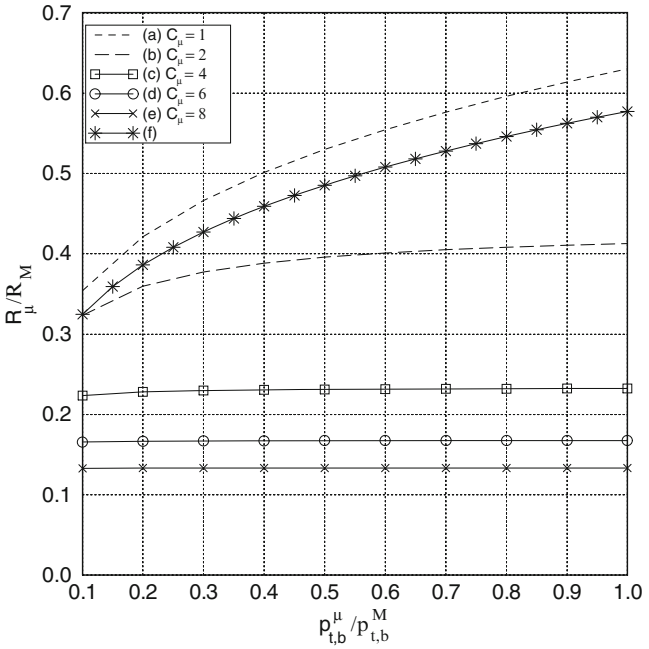

Fig. 11.19 Downlink microcell radius R_μ against $\Omega^\mu_{t,b}/\Omega^M_{t,b}$ for different values of C_μ in the case $\eta = 10\,\text{dB}$, $(C/I)_{req} = 18\,\text{dB}$, and $h^\mu_b/h^M_b = 1/3$, whereby the microcell radius is normalized with respect to the macrocell radius R_M; $\Omega^\mu_{t,b}/\Omega^M_{t,b}$ represents the ratio of the transmitted power of microcell BS to that of macrocell BS; C_μ is the number of clusters in a micro-area; η is the front-to-back ratio of the directional antenna; $h^\mu_b/h^M_{t,b}$ is the ratio of the microcell BS antenna to the macrocell BS antenna. Curves (a)–(e) are obtained by C/I-criterion for $C_\mu = 1, 2, 4, 6$, and 8, while curve (f) is obtained by C-criterion

(b) $C_\mu \geq 2$**:** Next, we consider the case where many microcells are deployed in each microarea. Figure 11.19 shows the downlink microcell size against $\Omega^\mu_{t,b}/\Omega^M_{t,b}$ for different values of C_μ, where $\Omega^\mu_{t,b}/\Omega^M_{t,b}$ is the ratio of the transmitted power of the microcell BS to that of the macrocell BS, and C_μ is the number of microcell clusters in a micro-area. It is observed that if $C_\mu \geq 3$, $\Omega^\mu_{t,b}/\Omega^M_{t,b}$ has little effect on the downlink microcell size. This is because the interference from the microcells, I^d_μ, will dominate the macrocell interference, J^d_μ, when the number of co-channel microcells $(C_\mu - 1)$ becomes large in a given micro-area. In other words, if a large number of microcells are installed, the C/I-criterion will become a dominating factor in determining the microcell size. In the case of $C_\mu = 6$, for example, one should follow the C/I-criterion to get $R_\mu \leq 0.165 R_M$ from Fig. 11.19.

Uplink Microcell Size

Similar to the previous analysis for the downlink microcell size, the uplink microcell size is derived from the C/I analysis. More specifically,

$$\frac{C_{\mu}^{\mathrm{u}}}{I_{\mu}^{\mathrm{u}}+J_{\mathrm{M}\mu}^{\mathrm{u}}}=\frac{\Omega_{\mathrm{t,m}}^{\mu}\dfrac{(h_{\mathrm{b}}^{\mu}h_{\mathrm{m}})^2}{R_{\mu,\mathrm{up}}^4}}{\displaystyle\sum_{i=1}^{C_{\mu}-1}\frac{\Omega_{\mathrm{t,m}}^{\mu}(h_{\mathrm{b}}^{\mu}h_{\mathrm{m}})^2}{D_{\mu_i}^4}+\sum_{i=1}^{N_{\mathrm{M_{f},}i}}\frac{\Omega_{\mathrm{t,m}}^{M}(h_{\mathrm{M}}^{\mathrm{b}}h_{\mathrm{m}})^2}{D_{\mathrm{M}_i}^4}}, \tag{11.26}$$

where the parameters $\Omega_{\mathrm{t,b}}^{\mu}$, $\Omega_{\mathrm{t,b}}^{\mathrm{M}}$, C_{μ} $h_{\mathrm{b}}^{\mathrm{M}}$, $D_{\mu,i}$, R_{M}, h_{b}^{μ}, and h_{m} have been defined in (11.11) and (11.17) and

$$\begin{aligned}
C_{\mu}^{\mathrm{u}} &= \text{microcell BS received power from the desired microcell MS}\\
I_{\mu M}^{\mathrm{u}} &= \text{uplink microcell-to-macrocell interference}\\
J_{\mathrm{M}\mu}^{\mathrm{u}} &= \text{uplink macrocell-to-microcell interference}\\
N_{\mathrm{M,f}} &= \text{the number of macrocell interfering MSs}\\
D_{\mathrm{M},i} &= \text{BS distance to the } i\text{-th interfering macrocell MS}\\
R_{\mu,\mathrm{up}} &= \text{uplink microcell radius}
\end{aligned}$$

Let $D_{\mathrm{M},i}=\widehat{D_{\mathrm{M},i}}R_{\mathrm{M}}$ and $(C/I)_{\mathrm{req}}$ denote the required C/I for a microcell BS. Using the same assumptions for getting (11.18), one can simplify (11.26) as

$$\frac{R_{\mu,\mathrm{up}}}{R_{\mathrm{M}}}\le\left(\frac{(C/I)_{\mathrm{req}}^{-1}}{\dfrac{(C_{\mu}-1)C_{\mu}^2}{9}+\left(\displaystyle\sum_{i=1}^{N_{\mathrm{M_f}}}\left(\frac{1}{\widehat{D_{\mathrm{M_{f},}i}}}\right)^4\right)\left(\dfrac{\Omega_{\mathrm{t,m}}^{\mathrm{M}}}{\Omega_{\mathrm{t,m}}^{\mu}}\right)}\right)^{\frac{1}{4}}. \tag{11.27}$$

We have shown that when the number of microcell clusters C_{μ} becomes large, the downlink microcell size is insensitive to the interference from the macrocells. This is also true for determining the uplink microcell size. This will be shown by a later example. When microcell interference dominates the performance, (11.27) can be approximated as

$$\frac{R_{\mu,\mathrm{up}}}{R_{\mathrm{M}}}\le\left(\frac{1}{(C/I)_{\mathrm{req}}\dfrac{(C_{\mu}-1)C_{\mu}^2}{9}}\right)^{\frac{1}{4}}. \tag{11.28}$$

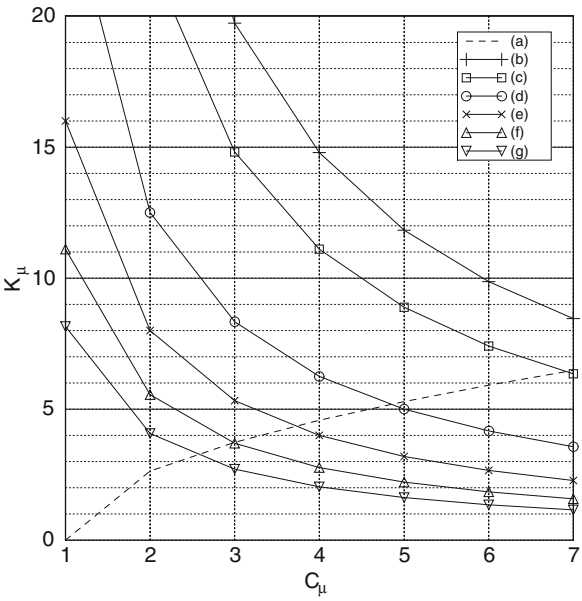

Fig. 11.20 K_μ against C_μ with R_μ/R_M as a parameter, whereby K_μ is the microcell cluster size, C_μ the number of clusters in a micro-area, and R_μ/R_M is the ratio of the microcell radius to the macrocell radius. Curve (a) represents the lower bound of K_μ, while curves (b)–(g) represent the upper bound of K_μ for $R_\mu/R_M = 0.13, 0.15, 0.20, 0.25, 0.30, 0.35$, respectively

By combining (11.19), (11.20), and (11.28), we obtain upper and lower bounds on K_μ as

$$\frac{1}{3}\sqrt{(C/I)_{\text{req}}(C_\mu - 1)} \le K_\mu \le \frac{1}{C_\mu}\left(\frac{R_M}{R_\mu}\right)^2. \tag{11.29}$$

The relation between K_μ and C_μ with R_μ/R_M as a parameter is shown in Fig. 11.20.

Example 11.3:

Consider again micro-area 56 in Fig. 11.14. Referring to Table 11.1, micro-area 56 can be assigned channel sets $[4_\alpha, 4_\gamma]$. Take channel set 4_α for example. The worst case interference occurs when interfering macrocell MSs transmit maximum power, i.e., at the macrocell boundary. For the example considered, the three first-tier interfering macrocell MSs near micro-areas 45, 47, and 77 are located at distances of $[\widehat{D_{M,1}}, \widehat{D_{M,2}}, \widehat{D_{M,3}}] = [2.0, 2.0, 2.0]$, respectively; the three second-tier interfering macrocell MSs near micro-areas 26, 53, and 89 are located at distances $[\widehat{D_{M,4}}, \widehat{D_{M,5}}, \widehat{D_{M,6}}] = [4.36, 4.36, 4.36]$, respectively; the three third-tier interfering macrocell MSs near micro-areas 32, 38, and 98 are located at distances $[\widehat{D_{M,7}}, \widehat{D_{M,8}}, \widehat{D_{M,9}}] = [6.0, 6.0, 6.0]$, respectively. Substituting these values into (11.27) and then letting $(C/I)_{\text{req}} = 18\,\text{dB}$, we show in Fig. 11.21 the ratio of microcell radius to macrocell radius R_μ/R_M against $\Omega^\mu_{t,m}/\Omega^M_{t,m}$ for different values of C_μ, where $\Omega^\mu_{t,m}/\Omega^M_{t,m}$ is the ratio of

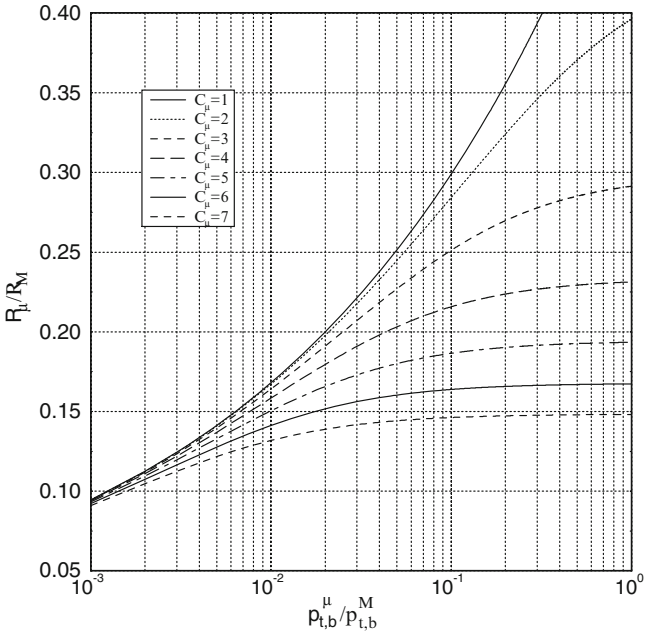

Fig. 11.21 Uplink microcell radius R_μ against $\Omega^\mu_{t,m}/\Omega^M_{t,m}$ for different values of C_μ, where the microcell radius is normalized by the macrocell radius R_M, $\Omega^\mu_{t,m}/\Omega^M_{t,m}$ is the ratio of the transmitted power of the microcell MS to that of the macrocell MS, C_μ is the number of microcell clusters in a micro-area, and $(C/I)_{req} = 18\,dB$

the transmitted power of the microcell MS to that of the macrocell MS, and C_μ is the number of the microcell clusters in a micro-area. It is shown that as C_μ increases, microcell size becomes insensitive to $\Omega^\mu_{t,m}/\Omega^M_{t,m}$.

Suppose our objective is to implement six microcell clusters in each macro-area (i.e. $C_\mu = 6$) and still maintain $(C/I)_{req} = 18\,dB$. We first need to know the feasible cluster size K_μ and the microcell radius. From Fig. 11.20, we obtain $K_\mu = 7$ and $R_\mu = 0.15 \times R_M$. Then from Fig. 11.21, we find the transmitted power for a microcell MS should be at least 0.017 times that for a macrocell MS. Consider an interfering macrocell MS which is transmitting at $-2\,dBW$. The microcell MS transmitted power should be larger than $-20\,dBW$ in this case. If the MS transmitted power ranges from $-22\,dBW$ to $-2\,dBW$ as was assumed earlier, then the MS can be used in both the macrocells and microcells of the cluster-planned architecture without changing the MS transmit power specification.

Table 11.3 Frequency management plan for avoiding adjacent channel interference

1α	1	22	43	64	85	106	127	148	169	190	211	232	253	274	295	316
2α	2	23	44	65	86	107	128	149	170	191	212	233	254	275	296	317
3α	3	24	45	66	87	108	129	150	171	192	213	234	255	276	297	318
4α	4	25	46	67	88	109	130	151	172	193	214	235	256	277	298	319
5α	5	26	47	68	89	110	131	152	173	194	215	236	257	278	299	320
6α	6	27	48	69	90	111	132	153	174	195	216	237	258	279	300	321
7α	7	28	49	70	91	112	133	154	175	196	217	238	259	280	301	322
1β	8	29	50	71	92	113	134	155	176	197	218	239	260	281	302	323
2β	9	30	51	72	93	114	135	156	177	198	219	249	261	282	303	324
3β	10	31	52	73	94	115	136	157	178	199	220	250	262	283	304	325
4β	11	32	53	74	95	116	137	158	179	200	221	251	263	284	305	326
5β	12	33	54	75	96	117	138	159	180	201	222	252	264	285	306	327
6β	13	34	55	76	97	118	139	160	181	202	223	253	265	286	307	328
7β	14	35	56	77	98	119	140	161	182	203	224	254	266	287	308	329
1γ	15	36	57	78	99	120	141	162	183	204	225	255	267	288	309	330
2γ	16	37	58	79	100	121	142	163	184	205	226	256	268	289	310	331
3γ	17	38	59	80	101	122	143	164	185	206	227	257	269	290	311	332
4γ	18	39	60	81	102	123	144	165	186	207	228	258	270	291	312	333
5γ	19	40	61	82	103	124	145	166	187	208	221	251	271	292	313	
6γ	20	41	62	83	104	125	146	167	188	209	222	252	272	293	314	
7γ	21	42	63	84	105	126	147	168	189	210	223	253	273	294	315	

11.4.3.4 Adjacent Channel Interference Analysis

To avoid excessive adjacent channel interference, it is desirable not to use the same channel sets in adjacent sectors. We will first review a frequency plan designed to avoid adjacent channel interference in the conventional macrocellular system. Then we will show that the same plan works for the cluster-planned hierarchical architecture. As shown in Fig. 11.10, a traditional 7/21 macrocellular system has 21 sectors. If the forward and reverse links each have 10 MHz of available spectrum, and the channel bandwidth is 30 kHz, then a total of 333 carriers can be assigned to the 21 sectors. A frequency plan that avoids adjacent channel interference is shown in Table 11.3 [153]. Each row in the table represents a frequency set that is designated to a sector. This scheme separates any two carriers assigned to adjacent sectors by seven carriers.

If the frequency plan in Table 11.3 is applied to the cluster-planned architecture in Fig. 11.14, there is no adjacent channel interference between macrocell sectors. Even with the addition of underlaid microcells, a two-carrier separation is maintained between the carriers assigned to the microcells and the co-site macrocells within a micro-area. For example, referring to Fig. 11.14 and Table 11.1, the channel set $[4\alpha, 4\gamma]$ is assigned to micro-area 56. The co-site macrocell sectors that use channel set $1\beta, 2\alpha$, and 7γ have at least a two-carrier separation. This feature is valid for all the micro-areas with channel assignment of Table 11.1.

11.5 Macrodiversity Architectures

Microscopic diversity techniques are used to combat the effects of envelope fading. Macrodiversity, or a large-scaled space diversity, has long been recognized as an effective tool to combat shadowing [134, 153], although it is effective against envelope fading as well. A TDMA macrodiversity system serves a mobile station (MS) simultaneously by several BSs. At any time, the BS with the best quality measure is chosen to serve the MS. The criterion for branch (or BS) selection is a key issue when designing a macrodiversity system. Usually, the branch selection is based on the local mean power rather than the instantaneous power [4, 5, 134, 255, 275, 299], because the branch selection algorithm cannot react to the rapidly varying instantaneous signal power. Here we focus on *local-mean-based* branch selection schemes.

Previous studies on macrodiversity systems have evaluated the co-channel interference performance with shadowing only [34, 273, 295] and shadowed Rayleigh fading channels [274]. The co-channel interference performance was also discussed in [162], but it was assumed that the branch selection was based on the instantaneous signal power. The error rate performance of macrodiversity systems has been analyzed in Gaussian noise with both shadowing and Rayleigh (or Nakagami) fading [4,5,255,256,299]. However, these studies did not consider co-channel interference. The analysis in [276] carries this further by considering the effect of Ricean fading on a local-mean-based macrodiversity system and by considering the correlation effect of the wanted signal at different branches of a macrodiversity system.

11.5.1 Co-channel Interference Outage

We now consider an analytical model for calculating the probability of co-channel interference outage, O_{I}, for an L-branch local-mean-based macrodiversity system with log-normal shadowing. The model assumes that the local mean envelope power of the desired signal, $\Omega_{\mathrm{d},k}$, is available for each branch k, where $k = 1, \ldots, L$. In practice, the desired signal power is mixed with the total interference power for each branch $\Omega_{\mathrm{I},k}$, so that $\Omega_{\mathrm{d},k} + \Omega_{\mathrm{I},k}$ is actually measured. However, the difference is small for large $\Omega_{\mathrm{d},k}/\Omega_{\mathrm{I},k}$. If the branch having the largest $\Omega_{\mathrm{d},k}$ is selected, then the local-mean envelope power of the selected branch is

$$\Omega_{\mathrm{d}} = \max\left(\Omega_{\mathrm{d},1}, \Omega_{\mathrm{d},2}, \cdots, \Omega_{\mathrm{d},L}\right). \tag{11.30}$$

Let $F_k(x)$ and $p_k(x)$ denote the cumulative distribution function (cdf) and the pdf of $\Omega_{\mathrm{d},k}$, respectively. If the $\Omega_{\mathrm{d},k}$ are treated as independent random variables with the

pdf in (2.292), then $\Omega_{\rm d}$ has the pdf $p_{\Omega_{\rm d}}(x) = L[F_k(x)]^{L-1}\, p_k(x)$. The probability of co-channel interference outage is

$$\begin{aligned} O_{\rm I} &= {\rm P}[\Omega_{\rm d}/\Omega_{\rm I} < \Lambda_{\rm th}] \\ &= 1 - \int_0^{\infty} \left(\int_{-\infty}^{x/\Lambda_{\rm th}} p_{\Omega_{\rm I}}(x)(y){\rm d}y \right) p_{\Omega_{\rm d}}(x){\rm d}x, \end{aligned} \tag{11.31}$$

where $\Omega_{\rm d}$ and $\Omega_{\rm I}$ are the total powers of the desired and interfering signals for the selected branch with pdfs $p_{\Omega_{\rm d}}(x)$ and $p_{\Omega_{\rm I}}(y)$, respectively, and $\Lambda_{\rm th}$ is the threshold C/I.

The interfering signals add noncoherently so that the total interference power on the kth branch is $\Omega_{I,k} = \sum_{i=1}^{N_{\rm I}} \Omega_{I,k,i}$, where $N_{\rm I}$ is the number of interferers and $\Omega_{I,k,i}$ is the power of the ith interferer on the kth branch. It is widely accepted that $\Omega_{{\rm I},k}$ can be approximated by a log-normal random variable with area mean power $\mu_{\Omega_{{\rm I},k}}$ and standard deviation $\sigma_{\Omega_{{\rm I},k}}$. As discussed in Sect. 3.1, the parameters $\sigma_{\Omega_{{\rm I},k}}$ and $\mu_{\Omega_{{\rm I},k}}$ can be calculated using a variety of methods, including the Fenton–Wilkinson and Schwartz and Yeh methods.

If the $\{\Omega_{{\rm I},k}\}_{k=1}^{n}$ are independent and identically distributed (i.i.d.), and the $\{\Omega_{d,k}\}_{k=1}^{L}$ are also i.i.d. and independent of the $\{\Omega_{{\rm I},k}\}_{k=1}^{n}$, then [273, 295]

$$\begin{aligned} O_{\rm I} = 1 - L \int_0^{\infty} & \left(\int_0^{x/\Lambda_{\rm th}} \frac{1}{\sqrt{2\pi}\sigma_{\Omega_{\rm I}}\xi y} \exp\left\{ \frac{-\left(10\log_{10}\{y\} - \mu_{\Omega_{\rm I}\,({\rm dB})}\right)^2}{2\sigma_{\Omega_{\rm I}}^2} \right\} {\rm d}y \right) \\ & \times \left(1 - Q\left(\frac{10\log_{10}\{x\} - \mu_{\Omega_{\rm d}\,({\rm dB})}}{\sigma_{\Omega_{\rm d}}} \right) \right)^{L-1} \\ & \times \frac{1}{\sqrt{2\pi}\sigma_{\Omega_{\rm d}}\xi x} \exp\left\{ \frac{-\left(10\log_{10}\{x\} - \mu_{\Omega_{\rm d}\,({\rm dB})}\right)^2}{2\sigma_{\Omega_{\rm d}}^2} \right\} {\rm d}x, \end{aligned} \tag{11.32}$$

where $\sigma_{\Omega_{\rm d}}$ and $\mu_{\Omega_{\rm d}({\rm dB})}$ are the shadowing standard deviation and area mean power of the desired signal on the kth diversity branch, respectively.

For ease of evaluation, we let $w = (10\log_{10}\{x\} - \ln\mu_{\Omega_{\rm d}\,({\rm dB})})/\sqrt{2}\sigma_{\Omega_{\rm d}}$ and transform (11.32) into a Hermite integration form. That is,

$$O_{\rm I} = 1 - \int_{-\infty}^{\infty} g(w){\rm e}^{-w^2}{\rm d}w \simeq 1 - \sum_{i=1}^{n} g(w_i)h_i, \tag{11.33}$$

where

$$\begin{aligned} g(w) = \frac{L}{\sqrt{\pi}} & \left(1 - Q\left(\frac{\sqrt{2}\sigma_{\Omega_{\rm d}}w + \xi\left(\mu_{\Omega_{\rm d}\,({\rm dB})} - \mu_{\Omega_{\rm I}\,({\rm dB})} - \Lambda_{{\rm th}({\rm dB})}\right)}{\sigma_{\Omega_{\rm I}}} \right) \right) \\ & \times \left(1 - Q\left(\sqrt{2}w\right) \right)^{L-1}, \end{aligned} \tag{11.34}$$

and w_i and h_i are the roots and weight factors of the nth-order Hermite polynomial, respectively [2].

11.5.2 Shadow Correlation

Until now, we have assumed independent shadowing on the macrodiversity branches. However, in many cases the macrodiversity branches will be correlated. Define

$$\Omega_d = \left(\Omega_{d,1}, \Omega_{d,2}, \cdots, \Omega_{d,L}\right). \tag{11.35}$$

For a correlated L-branch macrodiversity system, the joint pdf of Ω_d is [72]

$$p_{\Omega_d}(\mathbf{z}) = \frac{1}{\sqrt{(2\pi)^L \det(\mathbf{M})}\xi^L z_1 \cdots z_L} \exp\left\{-\frac{1}{2}\mathbf{Y}^{\mathrm{T}}\mathbf{M}^{-1}\mathbf{Y}\right\}, \tag{11.36}$$

where $\mathbf{z} = (z_1, \cdots, z_L)$, $\mathbf{Y}^{\mathrm{T}} = [y_1, \cdots, y_L]$ denotes the transpose of column vector

$$\mathbf{Y} = \begin{bmatrix} 10\log_{10}(z_1) - \mu_{\Omega_{d,1}\,(\mathrm{dB})} \\ \vdots \\ 10\log_{10}(z_L) - \mu_{\Omega_{d,L}\,(\mathrm{dB})} \end{bmatrix} \tag{11.37}$$

and $\mu_{\Omega_{d,1}\,(\mathrm{dB})}, \cdots, \mu_{\Omega_{d,L}\,(\mathrm{dB})}$ are the area means of each diversity branch. The covariance matrix $\mathbf{M}$ is expressed as

$$\mathbf{M} = \begin{bmatrix} \sigma^2_{\Omega_1} & \cdots & \nu_{1L} \\ \vdots & \ddots & \vdots \\ \nu_{L1} & \cdots & \sigma^2_{\Omega_L} \end{bmatrix}, \tag{11.38}$$

where σ_Ω is the shadowing standard deviation and ν_{ij} is the covariance of $\Omega_{d,i\,(\mathrm{dB})}$ and $\Omega_{d,j\,(\mathrm{dB})}$

$$\nu_{ij} = \mathrm{E}\left[\left(\Omega_{d,i\,(\mathrm{dB})} - \mu_{\Omega_{d,i}\,(\mathrm{dB})}\right)\left(\Omega_{d,j\,(\mathrm{dB})} - \mu_{\Omega_{d,j}\,(\mathrm{dB})}\right)\right]. \tag{11.39}$$

It is convenient to define $\mathbf{N} = \mathbf{M}^{-1}$ and express the matrix multiplication in (11.36) in the form

$$\mathbf{Y}^{\mathrm{T}}\mathbf{N}\mathbf{Y} = \sum_{i=1}^{L} N_{ii} y_i^2 + 2\sum_{i=1}^{L-1}\sum_{j=i+1}^{L} N_{ij} y_i y_j \tag{11.40}$$

where N_{ij} is the element in the ith row and jth column.

According to (11.30), (11.36) and (11.40), the probability that $\Omega_{\rm d} < y$ is

$$\mathrm{P}[\Omega_{\rm d} < y] = \int_0^y \cdots \int_0^y \frac{1}{\sqrt{(2\pi)^L \det(\mathbf{M})}\xi^L z_1 \cdots z_L} \times \exp\left\{-\frac{1}{2}\left(\sum_{i=1}^{L} N_{ii} y_i^2 + 2\sum_{i=1}^{L-1}\sum_{j=i+1}^{L} N_{ij} y_i y_j\right)\right\} \mathrm{d}\mathbf{z}, \quad (11.41)$$

where N_{ij} and y_i are defined in (11.40) and (11.37), respectively.

The key for obtaining the probability of co-channel interference outage of the local-mean-based macrodiversity system is to find the pdf of the combiner output power, $p_{\Omega_{\rm d}}(y)$. Unlike the uncorrelated case where there exists a closed-form expression for $p_{\Omega_{\rm d}}(y)$, one cannot easily get a simple closed formula for the joint distribution of more than two mutually correlated log-normal random variables. However, for $L = 2$ and $\mu_{\Omega_{d,j}\ (\rm dB)} = \mu_{\Omega_d\ (\rm dB)}$

$$\begin{aligned} p_{\Omega_{\rm d}}(z) = \frac{1}{\sqrt{2\pi \det(\mathbf{M})}\xi^2} \Bigg(& \frac{1}{\sqrt{N_{22}}} \exp\left\{-\frac{z^2}{2}\left(N_{11} - \frac{N_{12}}{N_{22}}\right)\right\} \\ & \times \left(1 - Q\left(\left(\sqrt{N_{22}} + \frac{N_{12}}{\sqrt{N_{22}}}\right) z\right)\right) \\ & + \frac{1}{\sqrt{N_{11}}} \exp\left\{-\frac{z^2}{2}\left(N_{22} - \frac{N_{12}}{N_{11}}\right)\right\} \\ & \times \left(1 - Q\left(\left(\sqrt{N_{11}} + \frac{N_{12}}{\sqrt{N_{11}}}\right) z\right)\right)\Bigg), \end{aligned} \quad (11.42)$$

where $z = (10\log_{10} y - \mu_{\Omega_{\rm d}\ (\rm dB)})$. Consider the following covariance matrix $\mathbf{M}$

$$\mathbf{M} = \begin{bmatrix} \sigma^2 & \nu \\ \nu & \sigma^2 \end{bmatrix} \quad (11.43)$$

and

$$\mathbf{N} = \mathbf{M}^{-1} = \frac{1}{\sigma^4 - \nu^2} \begin{bmatrix} \sigma^2 & -\nu \\ -\nu & \sigma^2 \end{bmatrix}. \quad (11.44)$$

By substituting (11.44) into (11.42), we express the pdf of the output local-mean power of the dual macrodiversity system as

$$p_{\Omega_{\rm d}}(y) = \frac{\sqrt{2}}{\sqrt{\pi}\sigma\xi^2 y}\left(1 - Q\left(\left(\frac{1-r}{\sqrt{1-r^2}}\right)\left(\frac{10\log_{10}y - \mu_{\Omega_{\rm d}\ ({\rm dB})}}{\sigma}\right)\right)\right.$$
$$\left. \times \exp\left\{-\frac{(10\log_{10}y - \mu_{\Omega_{\rm d}\ ({\rm dB})})^2}{2\sigma^2}\right\}\right), \qquad (11.45)$$

where the correlation coefficient r is defined as $r = \nu/\sigma^2$. Combining (11.31) and (11.45), gives

$$O_{\rm I} = 1 - \int_{-\infty}^{\infty} g(w)\mathrm{e}^{-w^2}\mathrm{d}w \simeq 1 - \sum_{i=1}^{n} g(w_i)h_i, \qquad (11.46)$$

where

$$g(w) = \frac{2}{\sqrt{\pi}}\int_{-\infty}^{\infty}\left(1 - Q\left(\frac{\sqrt{2}\sigma_{\rm d}w + [\mu_{\Omega_{\rm d}\ ({\rm dB})} - \mu_{\Omega_{\rm I}\ ({\rm dB})} - \Lambda_{\rm th\ (dB)}]}{\sigma_{\Omega_{\rm I}}}\right)\right)$$
$$\times\left(1 - Q\left(\frac{1-r}{\sqrt{1-r^2}}\sqrt{2}w\right)\right). \qquad (11.47)$$

11.5.3 Numerical Examples

Consider a cellular system with nine cells per cluster. In this case, two co-channel interferers are at $5.2R$, where R is the cell radius. Assume the mobile unit is on the boundary of the cell at a distance of R to the BS. Consider a dual slope path loss model with $a = b = 2$ and $g = 0.15R$ in (2.248).

Figure 11.22 shows the probability of co-channel interference outage performance, while Table 11.4 lists the threshold $\Lambda_{\rm th}$ and diversity gain (D.G.) in terms of 5% and 10% co-channel interference outage probabilities. Diversity gain here is defined as the additional C/I (in dB) that is required by a system without diversity to produce the same probability of co-channel interference outage. Some general observations can be made: (1) a higher shadowing spread leads to a higher diversity gain and a lower required threshold $\Lambda_{\rm th}$; (2) the diversity gain per branch is decreased as the number of diversity branches is increased; (3) the diversity gain increases with the requirement of the system, e.g., the diversity gain for a 5% outage probability is higher than that for a 10% outage probability.

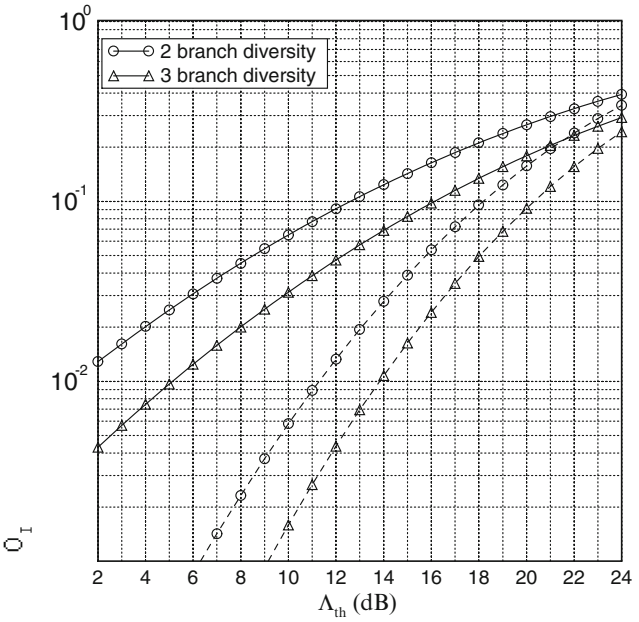

Fig. 11.22 Probability of co-channel interference outage, O_I, against the required threshold, Λ_{th}, at the receiver for the local-mean-based macrodiversity system, where the *solid lines* (——) denote the case for shadowing standard deviation $\sigma = 10$ dB and the *dashed lines* (– – –) for $\sigma = 6$ dB; $a = b = 2$, $g = 0.15R$; two interferers are located at a distance of $5.2R$

Table 11.4 Macrodiversity gain (D.G.) and the threshold Λ_{th} of C/I set at the receiver in terms of 5% and 10% probability of co-channel interference outage, O_I, over a pure shadowing channel; $\sigma = 6$ dB

	$O_I = 5\%$		$O_I = 10\%$	
L	Λ_{th}	D.G.	Λ_{th}	D.G.
1	10.96	–	13.69	–
2	15.78	4.82	18.12	4.43
3	17.97	7.01	20.46	11.78
4	19.41	8.45	21.80	13.13

We evaluate the effects of correlation coefficient r on a two-branch macrodiversity system with various σ; $\sigma = 6$ dB in Fig. 11.23 and $\sigma = 10$ dB in Fig. 11.24. With respect to a 10% outage, Table 11.5 lists Λ_{th} with different r. Observe that as r approaches unity, the diversity gain becomes zero. Furthermore, for $r = 0.7$, the diversity gain will be reduced to about 50% of the gain when $r = 0$.

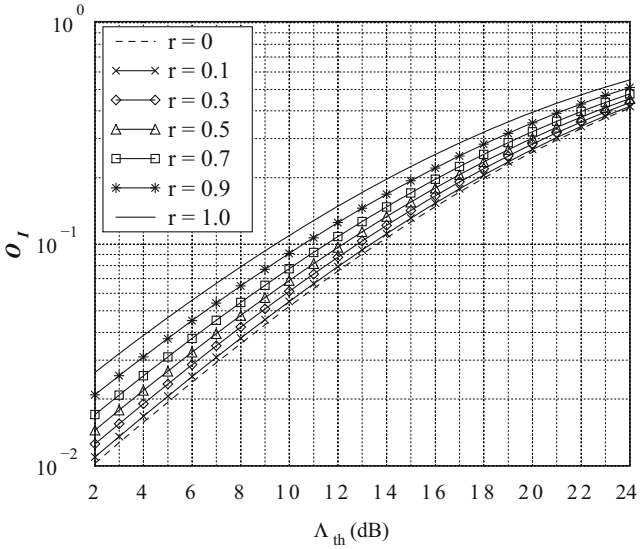

Fig. 11.23 Effect of branch correlation coefficient r on the local-mean-based macrodiversity system with $\sigma = 6\,\text{dB}$; $a = b = 2$, $g = 0.15R$; two interferers are located at a distance of $5.2R$

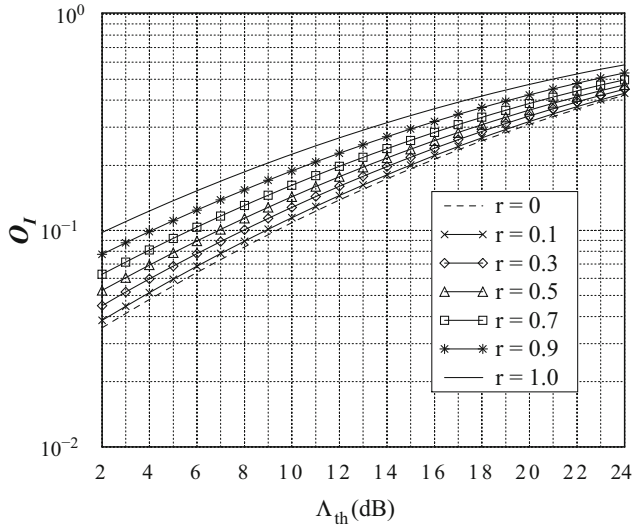

Fig. 11.24 Effect of branch correlation coefficient r on the local-mean-based macrodiversity system with $\sigma = 10\,\text{dB}$; $a = b = 2$, $g = 0.15R$; two interferers are located at a distance of $5.2R$

Table 11.5 Effects of branch correlation on a two-branch macrodiversity

	$\sigma = 6$ dB		$\sigma = 10$ dB	
r	Λ_{th}	D. G.	Λ_{th}	D. G.
0	13.54	3.99	9.24	6.96
0.1	13.39	3.84	8.93	6.65
0.3	12.78	3.23	7.94	5.66
0.5	12.23	2.68	7.00	4.72
0.7	11.46	1.91	5.67	3.39
0.9	10.51	1.02	4.12	1.84
1.0	9.55	–	2.28	–

Problems

11.1. Consider a regular hexagonal cell deployment, where the MSs and BSs use omnidirectional antennas. Suppose that we are interested in the forward channel performance and consider only the first tier of co-channel interferers as shown in Fig. 1.12. Ignore the effects of shadowing and multipath fading, and assume that the propagation path loss is described by the inverse β law in (1.5).

(a) Determine the worst case carrier-to-interference ratio, Λ, as a function of the reuse cluster size N, for $\beta = 3, 3.5$, and 4.
(b) What is the minimum cluster size that is needed if the radio receivers have $\Lambda_{th} = 9$ dB?
(c) Referring to Fig. 1.13, repeat parts (a) and (b) for the reverse channel.

Note: In this problem you must use exact radio path distances.

11.2. Consider a cellular system that uses a 7-cell hexagonal reuse cluster. The base stations use 120^o wide-beam directional antennas and they all have the same antenna height and transmit with the same power level. Consider the forward channel (base-to-mobile). Ignore shadowing and envelope fading and consider only the path loss. A mobile station will experience the lowest co-channel interference ratio, Λ, when it is located in the corner of a cell.

(a) Considering only the first tier of co-channel base stations, what is the worst case Λ with a path loss exponent of 4?
(b) Considering the first two tiers of co-channel base stations, what is the worst case Λ with path loss exponent of 4?
(c) From parts (a) and (b) what conclusions can you make about the effect of the second-tier co-channel base stations?
(d) What happens if the path loss exponent is equal to 3?

Note: In this problem you must use exact radio path distances.

11.3. A cellular network provider uses a TDMA scheme that can tolerate a C/I of 9 dB in the worst case. The propagation environment is characterized by a path loss exponent $\beta = 4$.

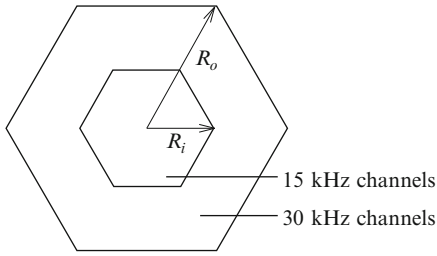

Fig. 11.25 Cell division with two-channel bandwidth scheme

(a) Find the best value of N for (1) omnidirectional antennas, (2) 120° sectoring, and (3) 60° sectoring.
(b) Suppose that the system bandwidth supports at total of N_{tot} voice channels. We wish to maximize the "cell capacity" defined as the number of voice channels per cell. Should sectoring be used?
(c) If sectoring is used, should you use 120° or 60° sectoring? Explain.

11.4. One method for improving the capacity of a cellular system uses a "two-channel bandwidth" scheme as suggested by Lee [154], where a hexagonal cell is divided into two concentric hexagons as shown in Fig. 11.25. The inner hexagon is serviced by 15 kHz channels, while the outer hexagon is serviced by 30 kHz channels. Suppose that the 30 kHz channels require $\Lambda = 18$ dB to maintain an acceptable radio link quality, while the 15 kHz channels require $\Lambda = 24$ dB.

Assume a fourth-law path loss model and suppose that the effects of envelope fading and shadowing can be ignored. Consider the mobile-to-base link and suppose that there are six co-channel interferers at distance D from the BS. For a 7-cell reuse cluster, it follows that the worst case carrier-to-interference ratio, Λ, when a mobile station (MS) is located at distance d from the BS is $\Lambda = (D/d)^4/6$. Hence, $\Lambda = 18$ dB requires $D/R_{\text{o}} = 4.6$, and $\Lambda = 24$ dB requires $D/R_{\text{i}} = 6.3$, where R_{i} and R_{o} are the radii of the inner and outer cells, respectively.

(a) Use the values of D/R_{i} and D/R_{o} to determine the ratio of the inner and outer cell areas, $A_{\text{i}}/A_{\text{o}}$.
(b) Let N_{i} and N_{o} be the number of channels that are allocated to the inner and outer portions of each cell, and assume that the channels are assigned such that $N_{\text{i}}/N_{\text{o}} = A_{\text{i}}/(A_{\text{o}} - A_{\text{i}})$. Determine the increase in capacity (as measured in channels per cell) over a conventional "one-channel bandwidth" system that uses only 30 kHz channels.

11.5. It has been suggested by [154] that the two-channel bandwidth scheme in Problem 11.4 can be combined with Halpern's reuse partitioning scheme. In this case, 15 kHz channels are used in the inner cells and 30 kHz channels are used in the outer cells. To have adequate performance in the inner or low bandwidth ring we must have $D_{\text{i}}/R_{\text{i}} = 6.3$, while the outer higher bandwidth ring can use $D_{\text{o}}/R_{\text{o}} = 4.6$.

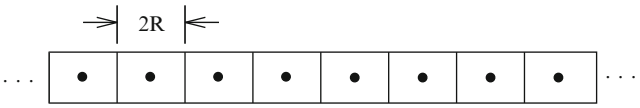

Fig. 11.26 Highway cell reuse pattern for Prob. 11.6

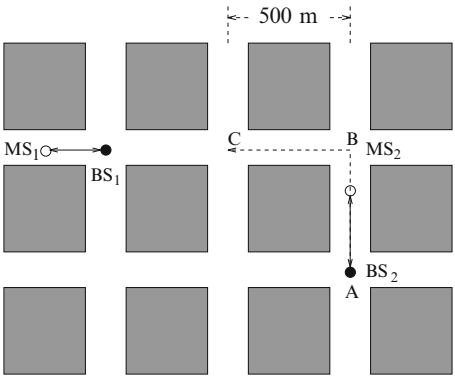

Fig. 11.27 Microcellular propagation environment for Prob. 11.7

Compute the increase in capacity (as measured in channels per cell) that will result from using this scheme, as compared to a conventional system using a 7-cell reuse cluster.

11.6. You are asked to design a highway cell reuse pattern as shown in Fig. 11.26 Each cell has length $2R$.

(a) A base station with an omnidirectional antenna is placed at the center of each cell. Shadowing is ignored under assumed line-of-sight conditions. Derive an expression for C/I in terms of the linear reuse cluster size N. Afterwards, determine the minimum reuse factor needed to yield a worst case carrier-to-interference ratio (C/I) of 9 dB or more. Consider only the nearest neighbouring co-channel interferers and assume a propagation path loss exponent $\beta = 4$.

(b) Now suppose that directional antennas are used to divide each cell into two semicircular sectors with boundaries perpendicular to the highway. Repeat part (a).

(c) Consider again the sectored cell arrangement in part (b). However, log-normal shadowing (due to heavy vehicle traffic) is now present with shadow standard deviation of σ_Ω dB. Derive an expression for the C/I outage on a cell boundary, again considering only the nearest neighbouring co-channel interferers.

11.7. Microcells are characterized by very erratic propagation environments. This problem is intended to illustrate the imbalance in the forward and reverse channel carrier-to-interference ratio that could occur in a street microcell deployment. Consider the scenario shown in Fig. 11.27 that consists of two co-channel BSs,

BS_1, and BS_2, communicating with two co-channel MSs, MS_1, and MS_2. Neglect the effects of shadowing and multipath, and assume that the non-line-of-sight corner path loss model in (2.351). Suppose that $a = 2$, $b = 4$, and $g = 150$ m. Plot Λ at BS_1, BS_2, MS_1, and MS_2 as MS_2 moves from A to C. When plotting your results, assume a received power level of 1 dBm at a distance of 1 m.